

Journal of Visualized Experiments

Quantification of Hydrogen Concentrations in Surface and Interface Layers and Bulk Materials through Depth Profiling with Nuclear Reaction Analysis

--Manuscript Draft--

Manuscript Number:	JoVE53452R3
Full Title:	Quantification of Hydrogen Concentrations in Surface and Interface Layers and Bulk Materials through Depth Profiling with Nuclear Reaction Analysis
Article Type:	Methods Article - JoVE Produced Video
Keywords:	hydrogen quantitation; depth profiling; surface hydrogen; bulk hydrogen; interface hydrogen; nuclear reaction analysis; ion beam analysis
Manuscript Classifications:	7.2.842.850: Surface Properties; 92.25.25: gas-surface interactions; 92.25.3: catalysts (chemical); 92.25.37: physical chemistry; 92.25.4: chemical analysis; 97.72.3: atomic beam measurements
Corresponding Author:	Markus Wilde, Dr. The University of Tokyo Tokyo, Tokyo JAPAN
Corresponding Author Secondary Information:	
Corresponding Author E-Mail:	wilde@iis.u-tokyo.ac.jp
Corresponding Author's Institution:	The University of Tokyo
Corresponding Author's Secondary Institution:	
First Author:	Markus Wilde, Dr.
First Author Secondary Information:	
Other Authors:	Shohei Ogura Katsuyuki Fukutani Hiroyuki Matsuzaki
Order of Authors Secondary Information:	
Abstract:	<p>Nuclear reaction analysis (NRA) via the resonant $1\text{H}(15\text{N},\alpha\gamma)12\text{C}$ reaction is a highly effective method of depth profiling that quantitatively and non-destructively reveals the hydrogen density distribution at surfaces, at interfaces, and in the volume of solid materials with high depth resolution. The technique applies a 15N ion beam of 6.385 MeV provided by an electrostatic accelerator and specifically detects the 1H isotope in depths up to about 2 micrometers from the target surface. Surface H coverages are measured with a sensitivity in the order of $\sim 10^{13} \text{ cm}^{-2}$ ($\sim 1\%$ of a typical atomic monolayer density) and H volume concentrations with a detection limit of $\sim 10^{18} \text{ cm}^{-3}$ ($\sim 100 \text{ at. ppm}$). The near-surface depth resolution is 2-5 nm for surface-normal 15N ion incidence onto the target and can be enhanced to values below 1 nm for very flat targets by adopting a surface-grazing incidence geometry. The method is versatile and readily applied to any high vacuum compatible homogeneous material with a smooth surface (no pores). Electrically conductive targets usually tolerate the ion beam irradiation with negligible degradation. Hydrogen quantitation and correct depth analysis require knowledge of the elementary composition (besides hydrogen) and mass density of the target material. Especially in combination with ultra-high vacuum methods for in-situ target preparation and characterization, $1\text{H}(15\text{N},\alpha\gamma)12\text{C}$ NRA is ideally suited for hydrogen analysis at atomically controlled surfaces and nanostructured interfaces. We exemplarily demonstrate here the application of 15N NRA at the MALT Tandem accelerator facility of the University of Tokyo to (1) quantitatively measure the surface coverage and the bulk concentration of hydrogen in the near-surface region of a H_2 exposed Pd(110) single crystal, and (2) to determine the depth location and layer density of hydrogen near the interface of a thin SiO_2 film</p>

	on Si(100).
Author Comments:	<p>Dear Dr. Nam and Mr. Solomon,</p> <p>I herewith resubmit our revised manuscript (JoVE 53452_R2_050515-W). I have followed your Editorial instructions and addressed the Reviewer's comments, hoping that the manuscript is now ready for publication in JoVE.</p> <p>As for the filming at the MALT accelerator facility, it will be necessary to schedule the filming during a time when the accelerator facility has assigned machine time to our group (Fukutani-Wilde Laboratory) for NRA measurements.</p> <p>Only during such times (typically 4-5 times per year for about one week) our group has access to the beamlines and we are able to use the accelerator for NRA measurements.</p> <p>The next opportunity to do so is a machine time from August 12 to August 21, 2015. The next machine time cannot be expected before October or November 2015. To proceed publication of our video article, I therefore suggest scheduling the filming during the upcoming August machine time. Please kindly consider whether a JoVE filming set can be arranged in this period.</p> <p>With very best regards, Markus Wilde</p>
Additional Information:	
Question	Response
If this article needs to be filmed by a certain date to due to author/equipment/lab availability, please indicate the date below and explain in your cover letter.	
If this article needs to be "in-press" by a certain date to satisfy grant requirements, please indicate the date below and explain in your cover letter.	

Markus Wilde* and Katsuyuki Fukutani
Institute of Industrial Science, The University of Tokyo
4-6-1 Komaba, Meguro-ku, 153-8505 Tokyo, Japan

March 20, 2015

Dear Editor of Journal of Visualized Experiments:

We herewith would like to submit our manuscript entitled “Quantification of Hydrogen Concentrations in Surface and Interface Layers and Bulk Materials through Depth Profiling with Nuclear Reaction Analysis” for publication in the Journal of Visualized Experiments.

In this article, we illustrate the application of $^1\text{H}(^{15}\text{N},\alpha\gamma)^{12}\text{C}$ resonant nuclear reaction analysis (NRA) in quantitative measurements of hydrogen densities on surfaces, in the volume, and at interfacial layers of solid materials. The ^{15}N NRA technique has many potential applications but there are only a few accelerator facilities worldwide where this method can be performed. Especially the combination with surface-analytical UHV instrumentation for the *in-situ* preparation of atomically controlled single crystal targets for hydrogen analysis at the MALT tandem accelerator facility of the University of Tokyo described herein is unique to our best knowledge. We believe that this highly versatile experiment deserves recognition by a wider audience and therefore chose to publish this work in JoVE. We were invited to submit our manuscript by Associate Editor Mathew Solomon.

As for the author contributions, M.W., S.O., and K.F. have been working together for more 15 years on the development of the ^{15}N NRA systems at MALT and performed over 110 machine times for NRA measurements at the facility in a large number of projects. This manuscript reflects much of the common experience in our team. M.W. acquired all NRA data and wrote the paper. H.M. is the head of the MALT facility and has provided generous support and assistance in the operation of the tandem accelerator.

We would like to suggest the following potential scientific reviewers for our manuscript:

Prof. William A. Lanford, SUNY at Albany
lanford@albany.edu

Prof. Klaus Christmann, Freie University Berlin

kchrchemie@fu-berlin.de

Prof. Yoshiaki Kido, Ritsumeikan University, Kusatsu, Shiga-ken 525-8577, Japan

ykido@se.ritsumei.ac.jp

Prof. Tetsuya Aruga, Kyoto University, Japan

aruga@kuchem.kyoto-u.ac.jp

Prof. Kenji Kimura, Kyoto University, Japan

kimura@kues.kyoto-u.ac.jp

Dr. Yousoo Kim, RIKEN, Japan

ykim@riken.jp

We hope that you will consider our manuscript suitable for publication in JoVE.

Sincerely Yours,

Markus Wilde

*Contact address: wilde@iis.u-tokyo.ac.jp (M. Wilde)

TITLE:

Quantification of Hydrogen Concentrations in Surface and Interface Layers and Bulk Materials through Depth Profiling with Nuclear Reaction Analysis

AUTHORS:

Wilde, Markus
Institute of Industrial Science
The University of Tokyo
Tokyo, Japan
wilde@iis.u-tokyo.ac.jp

Ogura, Shohei
Institute of Industrial Science
The University of Tokyo
Tokyo, Japan
ogura@iis.u-tokyo.ac.jp

Fukutani, Katsuyuki
Institute of Industrial Science
The University of Tokyo
Tokyo, Japan
fukutani@iis.u-tokyo.ac.jp

Matsuzaki, Hiroyuki
Micro Analysis Laboratory, Tandem accelerator, The University Museum
The University of Tokyo
Tokyo, Japan
hmatsu@um.u-tokyo.ac.jp

CORRESPONDING AUTHOR:

Wilde, Markus
Tel: +81-3-5452-6148
Fax: +81-3-5454-6159

KEYWORDS:

Hydrogen quantitation; depth profiling; surface hydrogen; bulk hydrogen; interface hydrogen; nuclear reaction analysis; ion beam analysis

SHORT ABSTRACT:

We illustrate the application of $^1\text{H}(^{15}\text{N},\alpha\gamma)^{12}\text{C}$ resonant nuclear reaction analysis (NRA) to quantitatively evaluate the density of hydrogen atoms on the surface, in the volume, and at an interfacial layer of solid materials. The near-surface hydrogen depth profiling of a Pd(110) single crystal and of $\text{SiO}_2/\text{Si}(100)$ stacks is described.

LONG ABSTRACT:

Nuclear reaction analysis (NRA) via the resonant $^1\text{H}(^{15}\text{N},\alpha\gamma)^{12}\text{C}$ reaction is a highly effective method of depth profiling that quantitatively and non-destructively reveals the hydrogen density distribution at surfaces, at interfaces, and in the volume of solid materials with high depth resolution. The technique applies a ^{15}N ion beam of 6.385 MeV provided by an electrostatic accelerator and specifically detects the ^1H isotope in depths up to about 2 micrometers from the target surface. Surface H coverages are measured with a sensitivity in the order of $\sim 10^{13} \text{ cm}^{-2}$ ($\sim 1\%$ of a typical atomic monolayer density) and H volume concentrations with a detection limit of $\sim 10^{18} \text{ cm}^{-3}$ ($\sim 100 \text{ at. ppm}$). The near-surface depth resolution is 2–5 nm for surface-normal ^{15}N ion incidence onto the target and can be enhanced to values below 1 nm for very flat targets by adopting a surface-grazing incidence geometry. The method is versatile and readily applied to any high vacuum compatible homogeneous material with a smooth surface (no pores). Electrically conductive targets usually tolerate the ion beam irradiation with negligible degradation. Hydrogen quantitation and correct depth analysis require knowledge of the elementary composition (besides hydrogen) and mass density of the target material. Especially in combination with ultra-high vacuum methods for *in-situ* target preparation and characterization, $^1\text{H}(^{15}\text{N},\alpha\gamma)^{12}\text{C}$ NRA is ideally suited for hydrogen analysis at atomically controlled surfaces and nanostructured interfaces. We exemplarily demonstrate here the application of ^{15}N NRA at the MALT Tandem accelerator facility of the University of Tokyo to (1) quantitatively measure the surface coverage and the bulk concentration of hydrogen in the near-surface region of a H_2 exposed Pd(110) single crystal, and (2) to determine the depth location and layer density of hydrogen near the interface of a thin SiO_2 film on Si(100).

INTRODUCTION:

The ubiquity of hydrogen as an impurity or as a constituent of a vast variety of materials and the wealth of hydrogen-induced interaction phenomena make revealing the hydrogen distribution in the near-surface region and at buried interfaces of solids an important task in many areas of engineering and fundamental material science. Prominent contexts include studies of hydrogen absorption in storage and purification materials for hydrogen energy applications, fuel cell, photo-, and hydrogenation catalysis, hydrogen retention and embrittlement in nuclear and fusion reactor engineering, hydrogen-induced surfactant effects in epitaxial growth fabrication and hydrogen-related electrical reliability issues in semiconductor device technology.

Despite its omnipresence and simple atomic structure, the quantitative detection of hydrogen poses analytical challenges. As hydrogen contains only a single electron, otherwise versatile elemental analysis by electron spectroscopy is rendered ineffective. Common hydrogen detection methods through mass analytical, optical, or nuclear resonance techniques such as metallurgical fusion, thermal desorption, infrared absorption or NMR spectroscopy are principally insensitive to the depth location of hydrogen. This precludes, e.g., discriminating between surface-adsorbed and bulk-absorbed hydrogen which differ substantially in their physical and chemical material interactions, and their distinction therefore becomes increasingly important for the analysis of nanostructured materials that comprise small volumes and large surface areas. Hydrogen profiling by secondary ion mass spectroscopy,

although providing depth-resolved quantitative H concentrations, is equally destructive to the analyzed target as metallurgical fusion, and sputtering effects may render the depth information obtained near the surface unreliable.

Nuclear reaction analysis with the narrow energy resonance (E_{res}) of the $^1\text{H}(^{15}\text{N},\alpha\gamma)^{12}\text{C}$ reaction at 6.385 MeV¹⁻³, on the other hand, combines the advantages of non-destructive hydrogen quantitation with high depth resolution in the order of a few nanometers near the surface. The method determines surface H coverages with a sensitivity in the order of 10^{13} cm^{-2} (~1% of a typical atomic monolayer density). Hydrogen concentrations in the interior of materials can be assessed with a detection limit of several 10^{18} cm^{-3} (~100 at. ppm) and a probing depth range of about 2 micrometers. The near-surface depth resolution is routinely 2–5 nm in surface-normal incidence of the ^{15}N ion beam onto the analyzed target. In surface-grazing incidence geometries, the resolution can be enhanced further to values below 1 nm. See Ref. 3 for a detailed account.

These capabilities have proven $^1\text{H}(^{15}\text{N},\alpha\gamma)^{12}\text{C}$ NRA as a powerful technique to elucidate the static and dynamic behavior of hydrogen at surfaces and interfaces in a large variety of processes and materials³. Established by Lanford⁴ in 1976, ^{15}N NRA was first used predominantly to quantitatively determine volume H concentrations in bulk materials and thin films. Among other purposes, the absolute hydrogen concentrations obtained through ^{15}N NRA have been used to calibrate other, not directly quantitative, hydrogen detection techniques^{5,6}. Also ^{15}N NRA hydrogen profiling in targets with well-defined interfaces in layered thin film structures has been described⁷⁻¹⁰. More recently, much progress has been achieved in studying hydrogen in the near-surface region of chemically clean and structurally well-defined targets by combining ^{15}N NRA with surface analytical ultra-high vacuum (UHV) instrumentation to prepare atomically controlled surfaces *in situ* for the H analysis³.

By quantifying the hydrogen coverage on single crystal surfaces, NRA has contributed significantly to the current microscopic understanding of hydrogen adsorption phases on many materials. $^1\text{H}(^{15}\text{N},\alpha\gamma)^{12}\text{C}$ NRA is furthermore the only experimental technique to directly measure the zero-point vibrational energy of surface-adsorbed H atoms¹¹, i.e., it can reveal the quantum-mechanical vibrational motion of adsorbed H atoms in the direction of the incident ion beam. Through the capability of nanometer-scale discrimination between surface-adsorbed and bulk-absorbed H, ^{15}N NRA can provide valuable insight into the hydrogen ingress through material surfaces, such as relevant to mineral hydration dating¹² or for observing hydride nucleation underneath surfaces of H-absorbing metals¹³⁻¹⁵. High-resolution ^{15}N NRA applications have demonstrated the potential to detect sub-monolayer thickness variations of adlayers¹⁶ and to distinguish surface-adsorbed from volume-absorbed hydrogen in Pd nanocrystals¹⁷. The combination with thermal desorption spectroscopy (TDS) allows for unambiguous identifications of H_2 thermal desorption features and for the depth-resolved assessment of the thermal stability of adsorbed and absorbed hydrogen states against desorption and diffusion^{13,15,18}. Due to its non-destructive nature and high depth resolution $^1\text{H}(^{15}\text{N},\alpha\gamma)^{12}\text{C}$ NRA is also the ideal method to detect hydrogen buried at intact interfaces, which allows for studying hydrogen trapping at metal/metal¹⁹⁻²² and metal/semiconductor interfaces

^{16,23-25} and for tracking hydrogen diffusion in stacked thin film systems⁹. By directly visualizing hydrogen redistribution phenomena between interfaces of SiO₂/Si-based metal-oxide-semiconductor (MOS) structures that relate to electrical device degradation, NRA has made particularly valuable contributions to device reliability research²⁶.

The hydrogen detection principle in NRA is to irradiate the analyzed target with a ¹⁵N ion beam of at least $E_{\text{res}}=6.385$ MeV to induce the resonant $^1\text{H}(^{15}\text{N},\alpha\gamma)^{12}\text{C}$ nuclear reaction between ¹⁵N and ¹H in the material. This reaction releases characteristic γ -rays of 4.43 MeV that are measured with a scintillation detector nearby the sample. The γ -yield is proportional to the H concentration in a certain depth of the target. Normalizing this signal by the number of incident ¹⁵N ions converts it into absolute H density after the γ -detection system has been calibrated with a standard target of known H concentration. ¹⁵N ions incident at E_{res} can react with hydrogen on the target surface. The concentration of buried hydrogen is measured with ¹⁵N ions incident at energies (E_i) above E_{res} . Inside the target material, the ¹⁵N ions suffer energy loss due to electronic stopping. This effect provides the high depth resolution, because the $^1\text{H}(^{15}\text{N},\alpha\gamma)^{12}\text{C}$ nuclear reaction resonance has a very narrow width (Lorentzian width parameter $\Gamma = 1.8$ keV) and the stopping power of materials for 6.4 MeV ¹⁵N ranges between 1-4 keV/nm, so that the passage of the ¹⁵N ion through only a few atomic layers is sufficient to shift its energy outside the resonance window. Thus, the resonant reaction detects buried H at $E_i > E_{\text{res}}$ in a probing depth $d=(E_i-E_{\text{res}})/S$, where S is the electronic stopping power of the analyzed material³.

By measuring the γ -yield while scanning the incident ¹⁵N ion energy in small increments, one obtains a nuclear reaction excitation curve that contains the density-depth distribution of hydrogen in the target. In this excitation curve (γ -yield vs. ¹⁵N energy), the actual H depth distribution is convolved with the NRA instrumental function that adds a predominantly Gaussian broadening and is the main limitation for the depth resolution³. At the surface (i.e., at $E_i = E_{\text{res}}$) the Gaussian width is dominated by a Doppler Effect due to zero-point vibration of the H atoms against the target surface.^{11,27,28} The yield curve of buried hydrogen detected at $E_i > E_{\text{res}}$ is affected by an additional Gaussian broadening component due to random ¹⁵N ion energy straggling inside the target. The straggling width increases in proportion to the square root of the ion trajectory length in the material^{29,30} and becomes the dominant resolution limiting factor above probing depths of 10-20 nm.

To demonstrate a few very typical hydrogen profiling applications with ¹⁵N NRA, we here exemplarily describe (1) the quantitative evaluation of the surface H coverage and of the bulk-absorbed hydrogen concentration in a H₂ exposed palladium (Pd) single crystal, and (2) the evaluation of the depth location and hydrogen layer densities at buried interfaces of SiO₂/Si(100) stacks. The NRA measurements are performed at the MALT 5 MV van-de-Graaf tandem accelerator³¹ of the University of Tokyo, which delivers a highly stable and well-monochromatized ($\Delta E_i \geq 2$ keV) ¹⁵N ion beam of 6 - 13 MeV. The authors have developed a computer control system for the accelerator to enable automated energy scanning and data acquisition for hydrogen profiling. Reflecting the two different NRA measurement tasks

presented by the above H profiling applications, the MALT facility provides two ion beam lines with specialized experimental stations: (1) a UHV surface analytical system with a single bismuth germanate (BGO, $\text{Bi}_4\text{Ge}_3\text{O}_{12}$) γ -scintillation detector dedicated to the NRA quantitation of hydrogen surface coverages, to zero-point vibration spectroscopy, and to H depth profiling at atomically controlled single crystal targets in a unique combination with TDS; and (2) a high vacuum chamber equipped with two BGO detectors positioned very close to the target for increased γ -detection efficiency, providing for a lower H detection limit and faster data acquisition. This setup has no sample preparation facilities but allows for rapid sample exchange (~ 30 min) and thus for a higher throughput of targets for which a well-controlled surface layer is not an essential part of the analytical task, such as H profiling at buried interfaces or the quantitation of bulk H concentrations. At both beam lines, the BGO detectors are placed conveniently outside of the vacuum systems because the γ -rays penetrate the thin chamber walls with negligible attenuation.

[Place Figure 1 here]

Figure 1 (A) illustrates the UHV system at beam line (BL)-1E, which is fully equipped for the *in-situ* preparation of atomically ordered single crystal surfaces and has a base pressure $<10^{-8}$ Pa to maintain surface cleanliness. To provide sample access for the surface-analytical tools, the 4" BGO scintillator is placed on the ^{15}N ion beam axis ~ 30 mm behind the target. The sample is mounted on a 4-axis manipulation stage for precise (x, y, z, θ) positioning and can be cooled with liquid nitrogen to ~ 80 K or with compressed He to ~ 20 K. Figure 1 (B) shows a Pd single crystal target mounted by spot-welded Ta support wires to a He compression cryostat. Quartz sheet spacers insulate the sample holder plate electrically from the cryostat body. This enables the incident ^{15}N ion beam current measurement necessary for quantitative NRA and allows for electron bombardment heating from the tungsten filament on the backside of the sample holder. A type K thermocouple is spot-welded to the edge of the Pd specimen. A quartz plate attached on the manipulator axis above the sample is used to monitor the ion beam profile and for sample-beam alignment. Figure 2 (A) shows the setup at BL-2C with two 4" BGO detectors arranged at 90° with respect to the ^{15}N beam with their front face no further than 19.5 mm apart from the beam axis. The sample holder (Figure 2 B) provides a simple clamping mechanism for quick sample exchange and allows for rotation of the sample around the vertical axis to adjust the ^{15}N incidence angle.

[Place Figure 2 here]

PROTOCOL:

1. Planning of Experiments

1.1) Identify the MALT accelerator beam line of interest depending on the measurement task (BL-1E for surface hydrogen, BL-2C for bulk or interfacial hydrogen). Contact the assisting scientist (currently M.W. or K.F.) to discuss details of the NRA measurements and their necessary preparations.

1.2) Download a beam time application form and observe the submission deadline on the MALT website³¹.

Note: The MALT facility invites new project proposals each March and September for the Summer (April-September) and Winter (October-March) half year terms, respectively.

1.3) Write the beam time proposal and submit as instructed on the MALT website.

1.4) After approval of the proposal, confirm the beam time schedule for the upcoming half year term as announced on the MALT website³¹. Safety training is required for new users in the beginning of the term.

1.5) Prepare for the beam time in advance. Consider all details of the experiment, and the time necessary for the transport of materials, for sample installation, and especially for *in-situ* surface preparation in UHV (if required). Ready the target specimen for the NRA measurement before the beam time starts.

2. Preparation for NRA Measurements at BL-1E (UHV)

Note: Always wear gloves when handling instruments and materials intended for use in vacuum, including the clean tools.

2.1) Install single crystal sample into UHV (refer to Figure 1 (B)).

2.1.1) Set spot-welder power to 3.5. Place single crystal specimen onto clean, flat, non-conducting working surface and spot-weld two 4-cm long pieces of tantalum (Ta) wire (0.3 mm diam.) in parallel to sample edges.

2.1.2) Gently bend wires to fit around the crystal edge shape while countering the bending forces with tweezers or pliers at the spot welding points. On a length of ~1 cm on each side, apply 2-4 additional spot welding points to the wire pair along the crystal edge.

2.1.3) Bend wire ends to point away from crystal center in a horizontal plane parallel to the working surface. Place sample with support wires onto the Ta plate (0.3 mm thick) of the sample holder. Align sample to cover the hole above the backside filament heater and fix the specimen position by spot-welding all four support wire ends onto the plate. If possible, apply more than one welding point to each wire end, moving from wire tip towards sample.

2.1.4) Cut away any excessive wire length standing out from holder plate edge. Set spot-welder power to minimum and release one pulse through spot-welding pliers closed empty. Spot-weld type K (chromel-alumel) thermocouple (0.2 mm diameter) to the upper edge of the crystal specimen.

2.1.5) Confirm proper connectivity of the sample mount by measuring resistances between the electrical feedthrough contacts at the cryostat head: Filament vs. sample (bias contact wire attached to sample holder plate) $> 20\text{ M}\Omega$; Filament vs. ground (cryostat body) $> 20\text{ M}\Omega$; Filament leads (0.3 mm diam. W) $< 3\text{ }\Omega$; Thermocouple leads: $\sim 16\text{ }\Omega$; Thermocouple vs. ground $> 20\text{ M}\Omega$; Thermocouple vs. sample $\sim 20\text{ }\Omega$ and $\sim 8\text{ }\Omega$ (depending on wire material, chromel or alumel).

2.1.6) Note distance between centers of sample and beam profile monitor (quartz plate).

2.1.7) Replace copper gasket on UHV manipulator head and carefully insert cryostat with mounted sample. Tighten flange bolts and evacuate UHV system following instructions from the assisting scientist.

2.1.8) Prepare UHV chamber for bake out by attaching heater tapes and aluminum foil. Assure normal operation of all turbo-molecular pumps for at least 30 min and a pressure $< 2 \times 10^{-4}\text{ Pa}$. Turn on chamber heaters to bake the UHV system for 24 hours.

2.1.9) Confirm ion gauge reading below $1 \times 10^{-5}\text{ Pa}$. Turn off baking heaters. Reactivate non-evaporable getter (NEG) pump with internal heater element at 400-450 °C for 30 min while the chamber is still hot.

2.1.10) Let chamber cool for 3-4 hours, then reattach QMS electronics and power supply cables to ion gun and LEED optics. Degas filaments of QMS, ion gun, and LEED. Confirm that chamber base pressure is $< 1 \times 10^{-8}\text{ Pa}$ after fully cooling to room temperature (within 12-24 hours).

2.2) Prepare single crystal surface in UHV (refer to Figure 1 (A)).

2.2.1) Position sample in chamber center with the manipulator x, y, z-stage and rotate to align surface between viewport and ion gun (facing the gas doser). Switch on ion gun power supply and adjust 'Emission' control to 20 mA. Look at the sample through the viewport and fine-adjust sample rotation angle so that the mirror image of the glowing ion gun filament is visible on the sample surface.

2.2.2) Set 'Beam energy' on ion gun power supply to 800 eV. Close NEG pump gate valve at the chamber bottom and introduce $6 \times 10^{-3}\text{ Pa}$ Ar gas into UHV chamber through variable leak valve. Confirm a sputter ion current (digital tester, from sample to ground) around $2\text{ }\mu\text{A}$ and sputter surface for 10 min at room temperature.

2.2.3) Add liquid nitrogen to the manipulator cryostat. At manipulator head, connect filament heater leads to power supply and digital tester (20 mV range) to thermocouple feedthrough. Ground the filament.

2.2.4) Connect sample contact to bias voltage power supply. Apply sample bias of 1 kV. Use filament heater currents up to 6.6 A for annealing, oxidation, and flash-heating in the next Step

(2.2.5) while monitoring the thermocouple voltage (sample temperature) with the digital tester.

CAUTION: NEVER touch digital tester or manipulator head while the sample is biased (risk of fatal electric shock!).

2.2.5) Anneal sample in UHV to 1000 K for 10 min ensuring the pressure remains below 2×10^{-7} Pa. Oxidize at 750 K in 5.0×10^{-5} Pa O_2 for 5 min, then reduce at room temperature (RT) in 5.0×10^{-5} Pa H_2 . Perform a final flashing to 600 K in UHV.

2.2.6) Observe LEED pattern and repeat steps 2.2.1) to 2.2.2) (sputtering) and 2.2.3.) to 2.2.5) (annealing/oxidation/ H_2 -reduction) until a clear (1×1) structure with bright spots on low background results (Figure 3) and no impurities remain in Auger electron spectroscopy³². Sputter for only 2-3 minutes in the repeated sputter/annealing cycles.

2.2.7) (optional) Add liquid nitrogen to the manipulator cryostat to cool sample to 90 K and expose to a few L of H_2 gas ($1 \text{ L} = 1.33 \times 10^{-4} \text{ Pa}\cdot\text{s}$). Perform a TDS measurement and finally verify that the H_2 thermal desorption spectrum conforms with literature data¹⁵.

Note: The preparations necessary in advance of the NRA beam time are now complete. The clean surface target can now be prepared routinely within ~2-3 hours by repeating Steps 2.2.1) through 2.2.6) with sputtering cycles of 2-3 minutes.

[Place Figure 3 here]

2.3) Align ^{15}N ion beam to single crystal target.

2.3.1.) At the 1E UHV chamber, position sample in chamber center ($x = 25$, $y = 26$, adjust z by eye to height of QMS front aperture) and rotate to face ^{15}N ion beam line. Bring quartz plate beam profile monitor (Figure 1 (B)) into NRA measurement position by lowering sample holder by sample-monitor distance measured in Step 2.1.5). Set digital camera on window flange below the manipulator to transmit beam profile image on the quartz plate to the TV monitor in the accelerator control room.

2.3.2) Remove all other electrical contacts to sample at manipulator head and connect signal line to digital current integrator in control room. Set electrostatic deflector voltage on BL-1E to 8500 V. Open the three manual gate valves on BL-1E between the UHV chamber and the bending magnet BM04.

2.3.3.) Obtain instructions from the assisting scientist to become familiar with the accelerator control system in the control room.

Note: Accelerator parameters (such as beam energy- and direction-defining magnet fields and focusing lenses) are set with assignable dials on a central control panel. Beam line valves and Faraday cups are remotely opened/closed by mouse clicks and pneumatic actuation.

2.3.4) In the control room, switch current integrator from 'Stand by' mode to 'Operate'. Connect integrator analog output to current indicator. At the accelerator control panel, adjust ^{15}N ion beam energy with accelerator in slit feedback mode to an energy analyzer magnet field of 5540 Gauss (Parameter: NMR03) and match bending magnet field (Parameter HPB04) to ~6033.4 Gauss to direct ion beam onto target in 1E UHV chamber. Set magnetic quadrupole lens parameters (MQ04) to XCC=4.64 A and YCC=5.15 A to focus beam approximately.

2.3.5) In the control room, open two gate valves between accelerator and beam line 1E. Open Faraday cup (FC) FC04 and observe ion beam profile on quartz plate in target chamber on the TV monitor. Fine tune BM04 and MQ04 parameter settings to obtain well-focused ion beam in center of profile monitor plate. Adjust z-position of quartz monitor with sample manipulator if necessary.

2.3.6) Close Faraday cup FC04 and lift up sample z-position again by sample-monitor distance. Take note of NMR03/HPB04/MQ04 (XCC, YCC) parameters and save them in a new MagparNNN.xls file for the current beam time (NNN, a three-digit number).

Note: Based on this reference NMR03/HPB04 input, MagparNNN.xls calculates the matching magnet field parameters for the energy-analyzing (BM03) and direction-switching (BM04) magnets necessary to keep the ion beam position on the target during a ^{15}N energy scan.

3. Preparation for NRA Measurement at BL-2C

3.1) Lift up any previously used sample from the beam line position into to the manipulator transfer rod, secure height with fixation screw, and close gate valve to the beam line.

3.2) Detach sample current line at electrical feedthrough and rotary pump line at KF flange coupling of the manipulator. Detach manipulator from the gate valve flange.

3.3) Place manipulator onto preparation table and slide sample holder out of the transfer tube. Rotate manipulator axis to place sample horizontally.

3.4) Loosen two M2 cap screws of sample clamp (Figure 2 (B)) and remove old target. Set new sample, align parallel to manipulator axis, and tighten clamp screws. Retract sample into transfer tube and secure position with fixation screw.

3.5) Replace copper gasket on gate valve and reinstall manipulator on the beam line. Attach rotary pump line to manipulator. Close valve in the rotary pump line to the turbo-molecular pump (TMP).

3.6) Open rotary pump line valve of the manipulator and evacuate transfer tube for 10-15 minutes to restore rotary base pressure. Close manipulator pump line valves and open valve in rotary pump line to TMP. Slowly open the gate valve to the manipulator and evacuate for 20-30

min to restore $2\text{--}3 \times 10^{-3}$ Pa.

3.7) Lower sample to beam line position and align surface normal of beam profile monitor (glass plate) to incident beam direction with aid of BL-2C camera and nearby TV monitor. Then connect BL-2C camera signal line to TV monitor in control room.

3.8) Connect sample current signal line between electrical feedthrough of sample manipulator and digital current integrator (control room). In the accelerator control room, switch current integrator from 'Stand by' mode to 'Operate' and connect integrator analog output to current monitor.

3.9) Roughly align ^{15}N ion beam to target in BL-2C by setting bending magnet field (Parameter HPB04) to ~ 0.6 Gauss (Polarity: positive), magnetic quadrupole lens MQ04 parameters to $\text{XCC}=4.64$ A and $\text{YCC}=5.15$ A, and quadrupole lens MQ-2C parameters $\text{A}=3.6$ A and $\text{B}=3.9$ A to focus beam approximately.

3.10) Fine-tune HPB04/MQ04(XCC, YCC)/MQ-2C(A, B) parameters to optimize beam transmission (unobstructed passage to target) and beam profile on target (use beam profile monitors BPM-1C and BPM-2C and BL-2C camera image) and take note of the best settings.

4. NRA Measurement at BL-1E

4.1) Flash-heat Pd sample to 600 K to free surface from any adsorbed contaminants. Stabilize sample temperature at 145 K with filament heater (~ 3.6 A) and running He compression cryostat (or liquid nitrogen cooling).

4.2) Close valves to accelerator and to NEG pump and expose sample to 2000 L H_2 (2.66×10^{-3} Pa $\times 100$ s) at 145 K. Let sample cool to 80 K and adjust a H_2 background pressure of 1×10^{-6} Pa.

4.3) In the control room, set ^{15}N ion beam energy at BM03 to desired start value for the energy scan (typically $\text{NMR03} = 5530$ Gauss) and adjust BM04 according to the MagparNNN.xls table.

4.4) Load the NRA data acquisition software (NRMain.vi) on the accelerator control PC at BL-2C. Select depth profiling routine 'AutoScanLinuxUHVfb3.vi'. In AutoScanLinuxUHVfb3.vi, push 'Read present values' to transfer current magnet parameter settings to the control PC software.

4.5) Verify again that all valves on BL-1E are open, that the sample current signal line is connected, that the current digitizer is set to 'Operate', and that a ^{15}N beam of ideally 15 ± 5 nA is available on FC04.

4.6) Set the stat START, STOP and STEP values of the BM03 parameter for the energy scan (typically 5530 Gauss, 5600 Gauss, and 1 Gauss, respectively) and turn the option 'Force TVC to gvm' on. For a ~ 15 nA beam of $^{15}\text{N}^{2+}$, set the 'Acquisition time' parameter to 50 s.

4.7) Click the 'Execution' arrow in AutoScanLinuxUHVfb3.vi console to start automated acquisition of a depth profile (up to ~35 nm depth in Pd for STOP = 5600 Gauss). At the end of the scan (or for an earlier termination), click 'Stop measurement' to close the data file.

4.8) Switch current digitizer to 'Stand by' mode, detach sample current line from sample manipulator feedthrough, and close the last gate valve on BL-1E before the UHV chamber.

4.9) Stop the background H₂ gas dosage by closing the variable leak valve. Open the NEG gate valve at the UHV chamber bottom. (Optional: Take a H₂ TDS spectrum of the sample).

4.10) For additional NRA measurements (optional), re-expose the Pd(110) surface to H₂ as instructed in 4.2) and repeat steps 4.3) through 4.9).

5. NRA Measurement at BL-2C

5.1) In the control room, set ¹⁵N ion beam energy at BM03 to desired START value for the energy scan (typically NMR03 = 5530 Gauss to start profiling at the surface).

5.2) Load the NRA data acquisition software (NRAMain.vi) on the accelerator control PC at BL-2C. Select depth profiling routine 'AutoScanLinux11.vi'. Enter the desired BM03 parameters for the automated energy scan (START, STOP, STEP), matching START to the BM03 value set in 5.1). For the present SiO₂/Si samples, set 'Acquisition time' to 50 s.

5.3) Verify again that all valves on BL-2C are open, that the sample current signal line is connected, that the current digitizer is set to 'Operate', and that a ¹⁵N²⁺ beam of 50-100 nA is available on FC04.

5.4) Click 'Execution' arrow in 'AutoScanLinux11.vi' to acquire a depth profile that terminates automatically at the STOP value of the BM03 parameter. At the end of the scan (or for earlier termination), click 'Stop measurement' to close the data file.

6. Data Analysis

6.1) Copy *.nra raw data files in /home/csadmin/DataTaking/BTNNN from the acquisition PC (NNN is the number of the current beam time) onto a USB memory stick and transfer to data analysis PC.

6.2) Start the home-built software package for NRA data analysis and open procedure 'NRA-Linux-2C-v3.ipf'. Obtain the procedures NRA-Analysis-2C-v4.ipf, LinuxAddOn-3-v3.ipf, and Menu-NRA.ipf and copy them to the data folder containing Igor User Routines.

6.3) Compile procedures and select 'Load NRA data' from the appearing 'NRA' menu. Select data file measured under 4.) or 5.) and click 'Continue' in the appearing pop-up dialog.

Note: The software generates two graph outputs from measured data: ‘raw data’ (raw γ -counts (*GRS*) vs. NMR03 magnet field as displayed during data acquisition), and ‘NRA spectrum’, corresponding to the excitation curve (background-subtracted and incident charge-normalized γ -yield (I_{norm}) vs. ^{15}N ion energy).

6.4) Select ‘Correct Sample Current readings’ from ‘NRA’ menu and choose the ‘Recalculate ISC (entire wave) from averaged ISC/IFar ratio (e.g., sample w/o bias)’ option from the drop down menu to rescale ion beam charge reading from current digitizer to actual dimension (μC), referenced to the averaged FC04 beam current readings of the entire data set. Delete the ‘Inorm_by_Faraday’ trace from the ‘NRA spectrum’ graph.

Note: Normalization to this scaled integrated incident charge is preferable (over normalization to the Faraday current) because it better reflects the ^{15}N ion charge that actually hits the target than the FC04 current. The latter is measured only once before the Faraday cup opens (to deliver the beam onto the target) and therefore does not account for beam current fluctuations that always occur to some degree during the acquisition time for each data point. Rescaling the sample charge is necessary because the current digitizer reading overestimates the actual incident ion beam charge due to secondary electron emission from the target.

6.5) Determine the NMR03 value corresponding to E_{res} (the maximum position of the surface resonance peak in the ‘raw data’ plot). If different from the software default value of 5535 Gauss, correct the entry (if necessary also the Stopping power value) by selecting ‘NMR, energy and depth scale’ routine from the ‘NRA’ menu.

6.6) If a background rate (cps) correction has become necessary, use first the ‘Correct Faraday readings’ function to recalculate the normalized γ -yield from the raw (*GRS*) data after revising the background value, entering a correction factor of 1 (for the FC04 current). Then run the ‘Correct Sample Current readings’ function again (Step 6.4) to recalculate also the charge-normalized γ -yield with the revised background in properly scaled relation to the FC04 Faraday.

6.7) Plot charge-normalized γ -yield vs. depth as top axis to display the convolved hydrogen depth distribution (Figure 4).

6.8) Add error bars to the graph using the respective function from the ‘NRA’ menu. Whenever possible, prefer charge-normalization.

Note: Counting statistics define the error ΔI of the NRA γ -yield, $I = GRS - \text{Background}$, through the error-propagated uncertainties of the measured raw counts, $\delta_{GRS} = \sqrt{GRS}$, and of the background, $\delta_{bg} = \sqrt{\text{Background rate (cps)} \times \text{Acquisition time}}$. ΔI hence calculates as: $\Delta I = \sqrt{(\delta_{GRS})^2 + (\delta_{bg})^2} = \sqrt{GRS + \text{Background rate (cps)} \times \text{Acquisition time}}$. The error bars in the depth profile graphs (Figures 4 and 5) are $\Delta I_{\text{norm}} = \Delta I / \text{incident ion beam charge}$.

6.9) (optional) Perform a fit analysis of the data with suitable model functions³.

REPRESENTATIVE RESULTS:

Figure 4 shows near-surface NRA H profiles of H₂-exposed Pd(110) measured in BL-1E UHV system at a sample temperature of 90 K under a H₂ background pressure of 1.33×10^{-6} Pa. The ¹⁵N ion incidence energy has been converted into probing depth using the stopping power of Pd ($S = 3.90$ keV/nm). The open symbol profile was obtained after pre-exposing the Pd(110) sample to 2000 L H₂ at 145 K to induce absorption of hydrogen into the Pd bulk¹⁵. This profile can be decomposed into a peak at $E_{\text{res}} = 6.385$ MeV and a broad γ -yield plateau stretching over the entire profiled depth region. The peak at E_{res} corresponding to H on the target surface, whereas the plateau region proves that hydrogen absorption into the Pd bulk has taken place. The surface peak has a nearly Gaussian shape. To demonstrate this better, Figure 4 includes two additional NRA excitation curves (gray and black solid symbols) that were recorded at 170 K under the same H₂ background pressure from a freshly prepared Pd(110) surface without H₂ pre-dosage. At this temperature only surface chemisorbed hydrogen is stable at Pd(110); any absorbed H would diffuse into the deeper bulk and escape from NRA detection in the near-surface region. Fitting the surface peak to a Gaussian profile yields a peak height of $I_{\text{max}} = 86.9 \pm 4.5$ cts/ μC and an $\text{FWHM} = 2\sqrt{\ln(2)} \cdot \sigma$ of 11.6 ± 0.4 keV, where σ is the Gaussian width parameter. From the Gaussian peak area $I_s = \sqrt{\pi} \cdot I_{\text{max}} \cdot \sigma$ and the γ -ray detection efficiency of the BL-1E setup (calibrated with a Kapton (C₂₂H₁₀O₅N₂)_n foil standard of precisely known H concentration ($c_{\text{bulk}} = 2.28 \times 10^{22}$ cm⁻³) and stopping power $S = 1.2879$ keV/nm) $\alpha = 7.56 \times 10^{-13}$ [(cts/ μC) \cdot keV \cdot cm²], one determines the absolute H density (N_s) on the H₂-exposed Pd(110) single crystal as $N_s = I_s / \alpha = 1.42 \times 10^{15}$ cm⁻². Relative to the Pd atom density on the Pd(110) surface of 9.35×10^{14} cm⁻² this corresponds to a H coverage of 1.52 ± 0.13 ML (monolayers), in very good agreement with the literature value (1.5 ML)^{15,33,34}.

Figure 4 also shows that the depth resolution of the NRA H profile in the near-surface region is limited by the width of the surface resonance peak to about 2-3 nm ($\approx \text{FWHM}/S$). Therefore, any abrupt features in the H profile such as the point-to-point γ -yield variations seen around 16 nm depth cannot correspond to actually existing steep H concentration gradients, because such would be smeared out by the surface peak width and additional energy broadening due to ¹⁵N ion straggling³. Hence, the γ -yield corrugations in the plateau region of the H profile (5 to 22 nm depth) reflect fluctuations of the BGO background count rate (separate background measurements confirm that such random fluctuations occur) and do not contain physical information on the depth distribution of the Pd-absorbed hydrogen. The latter distribution is expected to be rather smooth in the homogenous single crystal, where H diffusion is rapid (several 100 nm/s even at 145 K)^{3, 13, 15}. Thus, the approximately constant concentration of the bulk-absorbed hydrogen in the near-surface region of the Pd crystal after exposure to 2000 L H₂ at 145 K can be evaluated by fitting the plateau data in Figure 4 to a sigmoid function that rises to its half-height at E_{res} with the same width as the Gaussian surface peak³. This analysis determines the plateau height I_{bulk} to 15.4 ± 1.3 cts/ μC . With the Pd stopping power $S = 3.9$ keV/nm, one thus obtains the H bulk concentration as $c_{\text{bulk}} = I_{\text{bulk}} \cdot S / \alpha = 7.94 \times 10^{20}$ cm⁻³, or 1.2% of the atomic density in bulk Pd (the latter equation is also used to calibrate α after having measured I_{bulk} in the Kapton standard³). This bulk H concentration signifies that finely

distributed grains of Pd hydride (which has a H/Pd ratio of about 0.65 at this temperature) has nucleated in the near-surface region of the Pd crystal during its exposure to 2000 L (2.66×10^{-3} Pa x 100 s) H₂ at 145 K, because the H solubility in the dilute solid solution phase of Pd amounts to less than H/Pd = 5×10^{-4} at this temperature and H₂ pressure.

Figure 5 displays ¹⁵N NRA depth profiles from a series of SiO₂/Si(100) stacks as they can be measured at BL-2C. The SiO₂ films had thicknesses of 19.0, 30.0, and 41.5 nm³⁵. In addition to a peak of surface hydrogen at E_{res}, all profiles show a second peak in larger depth, indicating that the H distribution within the oxide film is apparently not uniform. The position of this second peak shifts to larger depth with increasing SiO₂ film thickness. The optically determined SiO₂ film thickness is indicated by vertical dashed lines in each panel (i)-(iii). Close inspection reveals that the center positions of the NRA profile peaks are located with a small offset of ~4 nm above the respective SiO₂/Si interfaces. This evidences that hydrogen tends to accumulate not exactly at but in a region extending over a few nm of the oxide in front of the interface. This peculiar H localization behavior has been attributed to the near-interfacial SiO₂ structure, where a large number of strain and sub-oxide³⁶ related defects provide preferential binding sites for hydrogen species³⁷. The strained interfacial region results from the reduction of the Si atom density by a factor of ~2 in the abrupt transition from crystalline Si to amorphous SiO₂. For quantitative evaluation the respective surface and near-interfacial peaks were fitted to Gaussian functions that are shown as solid lines in Figure 5. An analysis equivalent to the one described above for the surface H peak on Pd(100) reveals that the near-interfacial oxide regions of the SiO₂/Si(100) film stacks contained a H layer density of $(1.0\text{-}1.3) \times 10^{14}$ cm⁻².

Figure 1: NRA setup in the BL-1E UHV system. (A) Schematic top view into the BL-1E UHV system equipped with sputter ion gun, low energy electron diffraction (LEED), and Auger electron spectroscopy (AES) for the *in-situ* preparation of atomically ordered and chemically clean single crystal surface targets and combined NRA and TDS measurements with a quadrupole mass spectrometer (QMS) mounted on a linear translation stage. (B) Pd single crystal specimen attached on the sample holder of the cryogenic manipulator.

Figure 2: NRA setup at BL-2C. (A) Schematic top view into the high vacuum chamber at BL-2C equipped with two BGO γ-detectors close to the target position. (B) Sample holder with a large chip target of SiO₂/Si(100) clamped on. Fogging up this sample type with water vapor after the NRA analysis visualizes the spots that were irradiated by the ¹⁵N ion beam.

Figure 3: LEED pattern (223 eV) of the cleaned Pd(110) surface in the BL-1E UHV system. The clear (1 × 1) pattern with bright diffraction spots on a low background signifies an atomically well-ordered surface structure.

Figure 4: Near-surface NRA H profiles of Pd(110) obtained in the BL-1E UHV system under a H₂ background of 1.33×10^{-6} Pa. Open symbols: Pre-exposed to 2000 L H₂ at 145 K, NRA measured at 90 K. Filled grey and black symbols: Two profiles measured at 170 K without H₂ pre-dosage. Refer to the Note in Procedure Step 6.8 for the error bar calculation.

Figure 5: NRA H profile of three SiO₂ film on Si(100) measured in the BL-2C system. (a) NRA H-profiles for three SiO₂ films on Si(100) with thicknesses of (i) 19.0 nm, (ii) 30.0 nm, and (iii) 41.5 nm. SiO₂/Si(100) interface positions are indicated by dashed vertical lines. This figure has been adapted from Ref. ³⁵ with permission from AIP. Refer to the Note in Procedure Step 6.8 for the error bar calculation.

DISCUSSION:

Figure 4 demonstrates the efficient distinction and quantitation of surface-adsorbed from bulk-absorbed hydrogen through ¹⁵N NRA at the example of a Pd(110) single crystal in the BL-1E UHV system. The high reproducibility of the surface H peak in the three profiles attests to the reliability of the *in-situ* UHV sample preparation and to the non-destructive nature of the NRA measurement. The quantitative agreement of the determined H coverage with the expected atomic saturation density further shows the accuracy of the NRA measurement. Close comparison between the NRA profiles of H₂ pre-exposed Pd(110) (open symbols) and the two excitation curves of only surface hydrogen on Pd(110) (grey and black symbols) in Figure 4 shows that the surface peak in the former H profile tails asymmetrically towards the plateau of bulk-absorbed hydrogen in the topmost ~5 nm. Such subtle detail of potentially non-uniform hydrogen distributions closely below the surface can only be revealed through NRA. A similar H accumulation in a shallow subsurface region has also been observed in other metals (Pt, Ti)^{11, 14}. The origin of this particular H behavior in the subsurface region is presently not clarified but scientifically interesting with regard to properly understanding the peculiar hydrogen absorption properties of nanomaterials¹⁷ as opposed to extended bulk metals.

Several critical parameters should be observed in the Protocol in order to obtain high quality data such as those in Figure 4. The H₂ background pressure introduced in Step 4.2 (1×10^{-6} Pa) is a deliberate choice such as to stabilize the H-saturation coverage on the Pd surface by balancing NRA ion beam-induced H-desorption through H-readsorption from the H₂ gas on one hand, while at the same time avoiding H uptake into the Pd bulk by H₂ absorption, on the other. If the H₂ pressure was too high, H absorption during the NRA analysis would cause a gradual increase of the NRA signal at E_{res} , because the surface resonance peak overlaps with about 2 nm of the topmost Pd bulk region, where H may accumulate, especially at even lower temperatures than those in the experiments of Figure 4.^{13-15, 18} Thus, for H-absorbing materials such as Pd or Ti, the appropriateness of the H₂ background setting has to be verified by confirming that the γ -yield at E_{res} remains constant on the time scale required to measure the surface resonance profile. This complication does not arise for most materials that do not absorb hydrogen at low H₂ pressures. Here, quantitation of the surface H saturation coverage is easily confirmed by observing saturation of the γ -yield at E_{res} when the H₂ background pressure is stepwise increased (up to a maximum of 10^{-2} Pa tolerable by the vacuum pump system).

Observe further that the data in Figure 4 were taken with a ¹⁵N²⁺ beam current of 15 ± 5 nA (Step 4.5). This beam current has proven to be sufficiently high, on one hand, as to develop reasonably intense γ -signals from the saturated layer density of surface H atoms from the viewpoint of acceptable data statistics and overall measurement time, and also to be still sufficiently gentle, on the other hand, as to avoid excessive H desorption (which would again

require higher H₂ background pressure for compensation) and sample heating (which may cause modification of the H depth distribution by thermal diffusion).

Although the NRA technique is versatile and easily applied to determine H surface layer densities on most vacuum compatible solid materials, limitations arise with respect to the detection of especially weakly adsorbed H-species that may not be stable against desorption under the incident ¹⁵N ion beam irradiation even under loss-compensating H₂ gas background (< 10⁻² Pa). For example, the authors have not yet succeeded in observing surface H-species with desorption temperatures (TDS) below ~70 K with NRA. The tendency of H to desorb from the sample or to redistribute inside the target by diffusion under the ion beam varies strongly between different target materials and should be evaluated as part of any given analysis by monitoring the γ -yield at the probing depth of interest as a function of the ion beam dose. Without a compensating H₂ background as applied here to Pd(110) where H readsorbs readily, in many cases a more or less pronounced exponential decay of the H-signal can be observed. Measuring and extrapolating such H-loss functions to zero ¹⁵N exposure allows reproducing the original H density on or inside the target prior to perturbation by the ion beam (for details, see Ref. 3). If the target size permits, reducing the current density (nA/cm²) in the beam-irradiated surface spot by defocusing the ion beam with aid of the MQ04 magnetic lenses (Protocol Steps 2.3.5 and 3.10) may alleviate H losses during the analysis. In general, excessive ¹⁵N ion doses should be avoided as they may cause physical damage to the target surface in the form of defects, which can change the H adsorption (and absorption) properties. In case of single crystals, the LEED pattern of the surface and the shape of the H₂ TDS spectrum¹⁵ should therefore be checked regularly. If any anomaly is observed, re-prepare the surface freshly as instructed (for Pd(110)) in Protocol Steps 2.2.1) through 2.2.6).

Figure 5 demonstrated at the example of thin film SiO₂/Si(100) stacks that hydrogen depth profiling analysis by ¹⁵N NRA can straightforwardly determine the depth location of near-interfacial H layers and the H density therein without destroying the sample material. Note, however, that the H accumulation in the interfacial regions seen in the depth profiles may partially result from the NRA analysis itself, because the ¹⁵N ion irradiation can cause redistribution of hydrogen in the material. This is a well-known effect^{35,38-40} and any possible H relocation during the NRA analysis should be verified by measuring the H concentration evolution at the accumulation peak depth on a non-irradiated sample spot in the course of continued ¹⁵N ion irradiation. Although this beam-induced H relocation effect can make determining the original H distribution in a specimen somewhat more difficult, it can be exploited for analytical purposes in dielectric reliability research to evaluate H redistribution trends between intact interfaces of (model) MOS device structures, providing information on relative material-specific H mobilities.^{3, 26}

Regarding the H detection limit of the NRA measurement, we note that the setup in BL-2C with its larger BGO detection solid angle (Figure 2 (A) has a more than twice as large calibrated γ -detection efficiency factor ($\alpha_{2C} = 1.79 \times 10^{-19}$ (cts/ μ C) \cdot (keV/nm) \cdot cm³) as in BL-1E ($\alpha_{1E} = 7.56 \times 10^{-20}$ (cts/ μ C) \cdot (keV/nm) \cdot cm³)) and hence provides higher sensitivity, favorable for the measurement of low H concentrations in materials that do not require *in-situ* surface

preparation. The background count rate in our γ -detection system is currently ~ 0.1 cps, setting a detection limit for volume H concentrations in solids in the order of 100 ppm (several 10^{18} cm^{-3}) with a 100-nA beam of $^{15}\text{N}^{2+}$ at BL-2C. In the present examples, this increased sensitivity (in combination with a stronger ion beam), permitted measuring the surface and interfacial layer H densities in the SiO_2/Si stacks with the same acquisition time (50 s) as the about one order of magnitude larger surface H saturation layer on Pd(110) (compare vertical axis scales in Figs. 4 and 5). The required acquisition time is determined by the desired counting statistics, the given H density in, and the ^{15}N ion beam current tolerated by the target. The acquisition time also defines the time resolution for the observation of transiently evolving H densities such as upon adsorption, desorption, absorption, or diffusion of hydrogen on or in materials.

The higher vacuum base pressure at BL-2C ($\sim 1 \times 10^{-5}$ Pa) may cause deposition of H-containing contaminants from the residual gas onto the target surface during the NRA measurement⁴¹. This may result in large surface H peaks in the depth profiles that can overwhelm features of interest directly below the surface, similar (but worse than) as seen, e.g., in the overlap with the shallower SiO_2/Si interfacial peak in Figure 5 (i). A large H content in the surface layer also negatively affects the evaluation of small bulk H concentrations in large probing depths ($E_i > \sim 9$ MeV) by inducing γ -ray background due to non-resonant nuclear reaction yield⁴². Although the BL 2C system presently already features 10-cm thick lead (Pb) shielding blocks for the BGO detectors (not shown for clarity in Figure 2) that reduce the count rate of environmental γ -radiation background, further improvement of the H detection limit may be achieved by implementing anti-coincidence shielding for the detectors, which can reduce background signals due to highly penetrating cosmic muon radiation⁴³.

ACKNOWLEDGMENTS:

We greatly appreciate M. Matsumoto for implementing the software that enables the automated measurement of NRA H depth profiles by remotely controlling the MALT accelerator parameters from the data acquisition PC. We thank S. Ohno and K. Namba for skillfully performing Pd(110) sample preparations and NRA and TDS measurements at the BL-1E UHV system, and C. Nakano for technical assistance in the accelerator operation. The $\text{SiO}_2/\text{Si}(100)$ specimen is gratefully received as a courtesy of Z. Liu of NEC Corporation, Japan. This work is partially supported by Grants-in-Aid for Scientific Research (Grant numbers 24246013 and 26108705) of the Japan Society for the Promotion of Science (JSPS), as well as through a Grant-in-Aid for Scientific Research in Innovative Areas 'Material Design through Computics: Complex Correlation and Non-Equilibrium Dynamics' from the Ministry of Education, Culture, Sports, Science, and Technology of Japan.

DISCLOSURES:

The authors declare that they have no competing financial interests.

REFERENCES

- 1 Lanford, W. A. Analysis for hydrogen by nuclear-reaction and energy recoil detection. *Nucl. Instrum. Methods Phys. Res. B* **66** (1-2), 65-82, doi: 10.1016/0168-583x(92)96142-I

- (1992).
- 2 Lanford, W. A. Nuclear Reactions for Hydrogen Analysis. In: *Handbook of Modern Ion Beam Materials Analysis*. Tesmer, J. R. & Nastasi, M., eds., Chapter 8, 193-204, Materials Research Society, Pittsburgh, PA, (1995).
 - 3 Wilde, M. & Fukutani, K. Hydrogen detection near surfaces and shallow interfaces with resonant nuclear reaction analysis. *Surf. Sci. Rep.* **69** (4), 196-295, doi: <http://dx.doi.org/10.1016/j.surfrep.2014.08.002> (2014).
 - 4 Lanford, W. A., Trautvetter, H. P., Ziegler, J. F. & Keller, J. New precision technique for measuring concentration versus depth of hydrogen in solids. *Appl. Phys. Lett.* **28** (9), 566-568, doi: 10.1063/1.88826 (1976).
 - 5 Ross, R. C., Tsong, I. S. T., Messier, R., Lanford, W. A. & Burman, C. Quantification of hydrogen in a-Si-H films by IR spectrometry, N-15 nuclear-reaction, and SIMS. *J. Vac. Sci. Technol.* **20** (3), 406-409, doi: 10.1116/1.571478 (1982).
 - 6 Suzuki, T., Konishi, J., Yamamoto, K., Ogura, S. & Fukutani, K. Practical IR extinction coefficients of water in soda lime aluminosilicate glasses determined by nuclear reaction analysis. *J. Non-Cryst. Solids* **382** (0), 66-69, doi: <http://dx.doi.org/10.1016/j.jnoncrsol.2013.10.011> (2013).
 - 7 Wagner, W., Rauch, F. & Bange, K. Concentration profiles of hydrogen in technical oxidic thin-films and multilayer systems. *Fresenius Z. Analyt. Chem.* **333** (4-5), 478-480, doi: 10.1007/bf00572357 (1989).
 - 8 Wagner, W., Rauch, F., Ottermann, C. & Bange, K. In-depth profiling of hydrogen in oxidic multilayer systems. *Surf. Interf. Anal.* **16** (1-12), 331-334, doi: 10.1002/sia.740160170 (1990).
 - 9 Wagner, W., Rauch, F., Ottermann, C. & Bange, K. Hydrogen dynamics in electrochromic multilayer systems investigated by the N-15 technique. *Nucl. Instrum. Methods Phys. Res. B* **50** (1-4), 27-30, doi: 10.1016/0168-583x(90)90323-m (1990).
 - 10 Hjörvarsson, B., Rydén, J., Karlsson, E., Birch, J. & Sundgren, J. E. Interface effects of hydrogen uptake in Mo/V single-crystal superlattices. *Phys. Rev. B* **43** (8), 6440-6445, doi: <http://dx.doi.org/10.1103/PhysRevB.43.6440> (1991).
 - 11 Fukutani, K., Itoh, A., Wilde, M. & Matsumoto, M. Zero-Point Vibration of Hydrogen Adsorbed on Si and Pt Surfaces. *Phys. Rev. Lett.* **88** (11), 116101, doi: <http://dx.doi.org/10.1103/PhysRevLett.88.116101> (2002).
 - 12 Ericson, J. E., Dersch, O. & Rauch, F. Quartz hydration dating. *J. Archaeological Sci.* **31** (7), 883-902, doi: 10.1016/j.jas.2003.12.004 (2004).
 - 13 Wilde, M., Matsumoto, M., Fukutani, K. & Aruga, T. Depth-resolved analysis of subsurface hydrogen absorbed by Pd(100). *Surf. Sci.* **482-485** (Part 1), 346-352, doi: 10.1016/s0039-6028(01)00727-0 (2001).
 - 14 Wilde, M. *et al.* Hydrogen sorption by Ti(0001) single crystal surfaces. *J. Vac. Soc. Jpn.* **45** (5), 458-462, doi: <http://dx.doi.org/10.3131/jvsj.45.458> (2002).
 - 15 Ohno, S., Wilde, M. & Fukutani, K. Novel insight into the hydrogen absorption mechanism at the Pd(110) surface. *J. Chem. Phys.* **140** (13), 134705, doi: <http://dx.doi.org/10.1063/1.4869544> (2014).
 - 16 Fukutani, K., Wilde, M. & Matsumoto, M. Nuclear-reaction analysis of H at the Pb/Si(111) inter-face: Monolayer depth distinction and interface structure. *Phys. Rev. B*

- 64** (24), 245411, doi: 10.1103/PhysRevB.64.245411 (2001).
- 17 Wilde, M., Fukutani, K., Naschitzki, M. & Freund, H. J. Hydrogen absorption in oxide-supported palladium nanocrystals. *Phys. Rev. B* **77** (11), 113412, doi: 10.1103/PhysRevB.77.113412 (2008).
- 18 Wilde, M. & Fukutani, K. Penetration mechanisms of surface-adsorbed hydrogen atoms into bulk metals: Experiment and model. *Phys. Rev. B* **78** (11), 115411, doi: 10.1103/PhysRevB.78.115411 (2008).
- 19 Okada, M., Nakamura, M., Moritani, K. & Kasai, T. Dissociative adsorption of hydrogen on thin Au films grown on Ir(111). *Surf. Sci.* **523** (3), 218-230, doi: [http://dx.doi.org/10.1016/S0039-6028\(02\)02408-1](http://dx.doi.org/10.1016/S0039-6028(02)02408-1) (2003).
- 20 Okada, M. *et al.* Reactivity of gold thin films grown on iridium: Hydrogen dissociation. *Appl. Catal. A General* **291** (1-2), 55-61, doi: 10.1016/j.apcata.2005.02.040 (2005).
- 21 Okada, M. *et al.* Reactive gold thin films grown on iridium. *Appl. Surf. Sci.* **246** (1-3), 68-71, doi: 10.1016/j.apsusc.2004.10.051 (2005).
- 22 Ogura, S. *et al.* Hydrogen adsorption on Ag and Au monolayers grown on Pt(111). *Surf. Sci.* **566-568** (Part 2), 755-760, doi: 10.1016/j.susc.2004.06.008 (2004).
- 23 Fukutani, K. *et al.* Interface hydrogen between a Pb overlayer and H-saturated Si(111) studied by a resonant nuclear reaction. *Surf. Sci.* **377** (1-3), 1010-1014, doi: 10.1016/S0039-6028(96)01536-1 (1997).
- 24 Fukutani, K., Iwai, H., Murata, Y. & Yamashita, H. Hydrogen at the surface and interface of metals on Si(111). *Phys. Rev. B* **59** (20), 13020-13025, doi: 10.1103/PhysRevB.59.13020 (1999).
- 25 Wilde, M. & Fukutani, K. Low-temperature growth of Au on H-terminated Si(111): Instability of hydrogen at the Au/Si interface revealed by non-destructive ultra-shallow H-depth profiling. *Jpn. J. Appl. Phys.* **42** (7B), 4650-4654, doi: 10.1143/jjap.42.4650 (2003).
- 26 Liu, Z., Fujieda, S., Ishigaki, H., Wilde, M. & Fukutani, K. Current Understanding of the Transport Behavior of Hydrogen Species in MOS Stacks and Their Relation to Reliability Degradation. *ECS Transactions* **35** (4), 55-72, doi: 10.1149/1.3572275 (2011).
- 27 Zinke-Allmang, M. & Kalbitzer, S. A novel method to determine vibrational energy states of atomic systems. *Z. Physik A* **323** (2), 251-252, doi: 10.1007/bf01290321 (1986).
- 28 Zinke-Allmang, M., Kalbitzer, S. & Weiser, M. Nuclear reaction spectroscopy of vibrational modes of solids. *Z. Physik A* **325** (2), 183-191, doi: 10.1007/bf01289649 (1986).
- 29 Bohr, N. K. *Dan. Vidensk. Selsk. Mat.-Fys. Medd.* **18** (1948).
- 30 Rud, N., Bøttiger, J. & Jensen, P. S. Measurements of energy-loss distributions for 6.5 MeV ^{15}N ions in solids. *Nucl. Instrum. Methods* **151** (1-2), 247-252, doi: 10.1016/0029-554X(78)90496-2 (1978).
- 31 MALT, <<http://malt.n.t.u-tokyo.ac.jp/index.html>>
- 32 Briggs, D. & Seah, M. P. *Practical Surface Analysis by Auger and X-ray Photoelectron Spectroscopy*. John Wiley & Sons, Chichester, (1983).
- 33 Rieder, K. H., Baumberger, M. & Stocker, W. Selective Transition of Chemisorbed Hydrogen to Subsurface Sites on Pd(110). *Phys. Rev. Lett.* **51** (19), 1799-1802, doi: <http://dx.doi.org/10.1103/PhysRevLett.51.1799> (1983).

- 34 Dong, W., Ledentu, V., Sautet, P., Kresse, G. & Hafner, J. A theoretical study of the H-induced reconstructions of the Pd(110) surface. *Surf. Sci.* **377–379** (0), 56-61, doi: 10.1016/s0039-6028(96)01349-0 (1997).
- 35 Wilde, M. *et al.* Influence of H₂-annealing on the hydrogen distribution near SiO₂/Si(100) interfaces revealed by in situ nuclear reaction analysis. *J. Appl. Phys.* **92** (8), 4320-4329, doi: 10.1063/1.1509084 (2002).
- 36 Himpsel, F. J., McFeely, F. R., Taleb-Ibrahimi, A., Yarmoff, J. A. & Hollinger, G. Microscopic structure of the SiO₂/Si interface. *Phys. Rev. B* **38** (9), 6084-6096, doi: <http://dx.doi.org/10.1103/PhysRevB.38.6084> (1988).
- 37 Helms, C. R. & Poindexter, E. H. The silicon-silicon dioxide system: Its microstructure and imperfections. *Rep. Progr. Phys.* **57** (8), 791, doi: 10.1088/0034-4885/57/8/002 (1994).
- 38 Briere, M. A., Wulf, F. & Braunig, D. Measurements of the accumulation of hydrogen at the silicon-silicon-dioxide interface using nuclear reaction analysis. *Nucl. Instrum. Methods Phys. Res. B* **45** (1-4), 45-48, doi: 10.1016/0168-583x(90)90781-o (1990).
- 39 Ecker, K. H., Krauser, J., Weidinger, A., Weise, H. P. & Maser, K. Nuclear reaction analysis of hydrogen migration in silicon dioxide films on silicon under N-15 ion irradiation. *Nucl. Instrum. Methods Phys. Res. B* **161-163** (0), 682-685, doi: 10.1016/s0168-583x(99)00830-7 (2000).
- 40 Maser, K. *et al.* Hydrogen migration in wet-thermally grown silicon dioxide layers due to high dose ¹⁵N ion beam irradiation. *Microelectron. Eng.* **48** (1-4), 139-142, doi: 10.1016/s0167-9317(99)00356-1 (1999).
- 41 Bugeat, J. P. & Ligeon, E. Influence of ion beam bombardment in hydrogen surface layer analysis. *Nucl. Instrum. Methods* **159** (1), 117-124, doi:doi: 10.1016/0029-554x(79)90337-9 (1979).
- 42 Wilde, M. & Fukutani, K. Evaluation of non-resonant background in hydrogen depth profiling via ¹H(¹⁵N,αγ)¹²C nuclear reaction analysis near 13.35 MeV. *Nucl. Instrum. Methods Phys. Res. B* **232** (1-4), 280-284, doi:doi: 10.1016/j.nimb.2005.03.058 (2005).
- 43 Horn, K. M. & Lanford, W. A. Suppression of background radiation in BGO and NaI detectors used in nuclear reaction analysis. *Nucl. Instrum. Methods Phys. Res. B* **45** (1-4), 256-259, doi:doi: 10.1016/0168-583x(90)90830-n (1990).

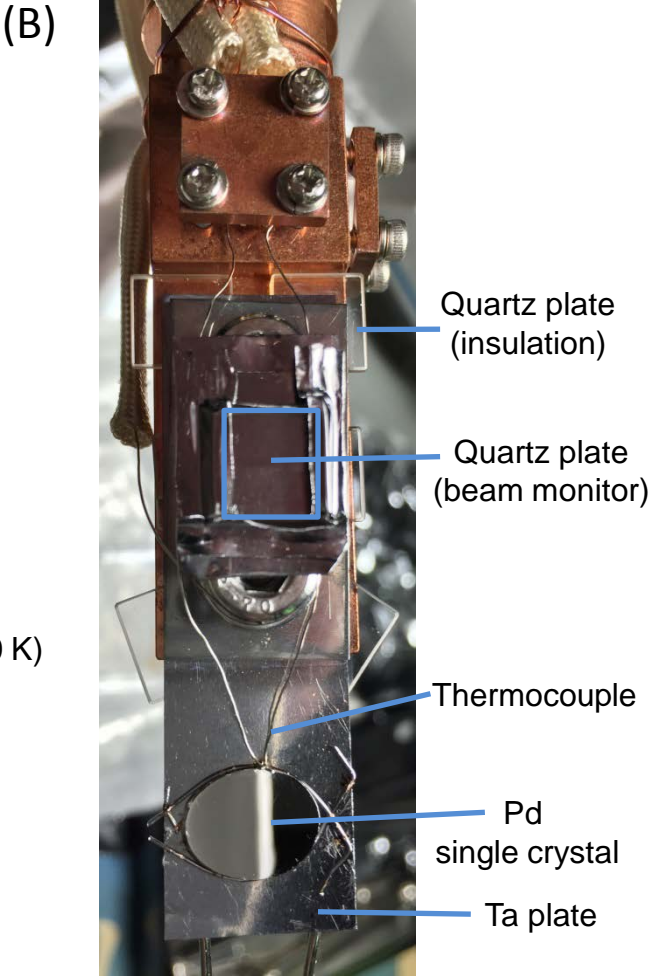
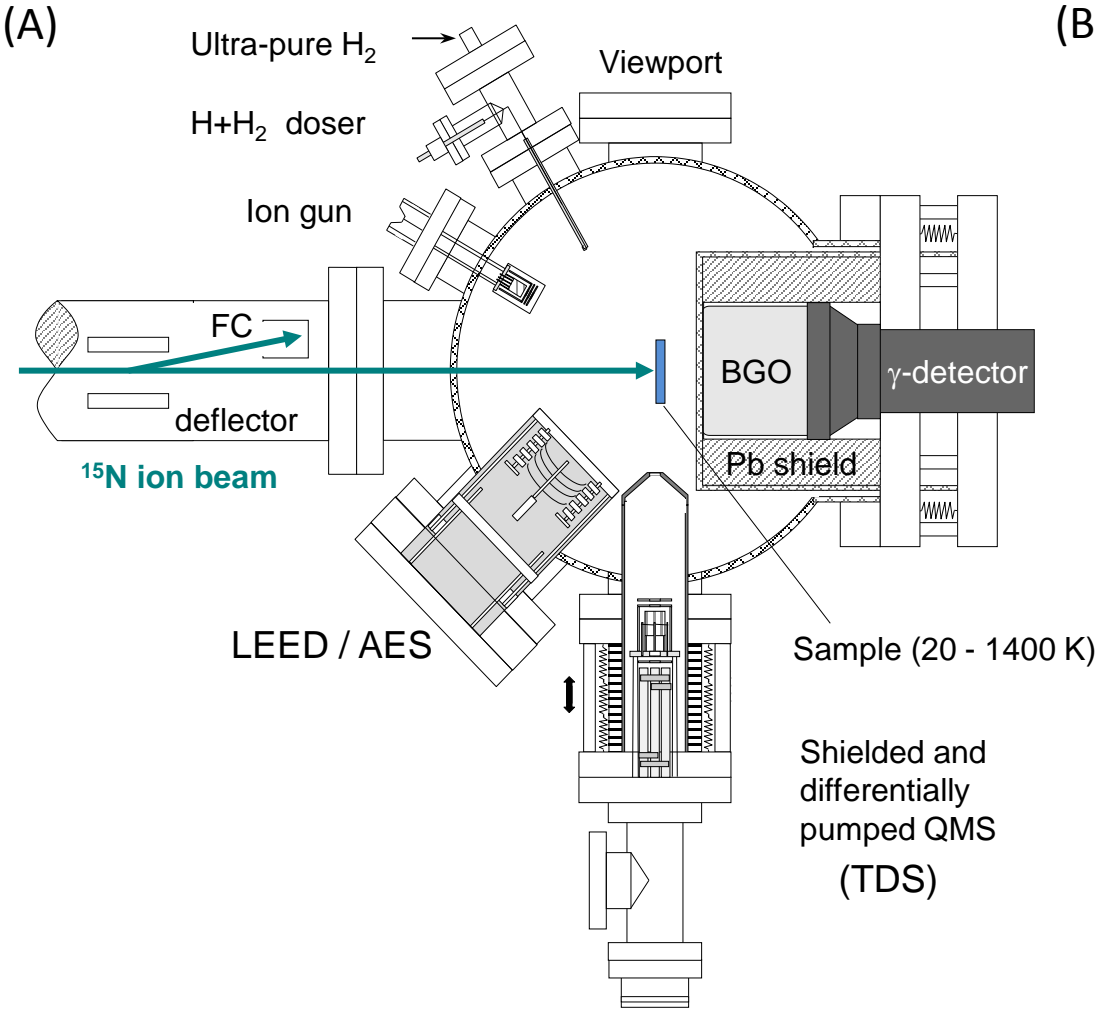
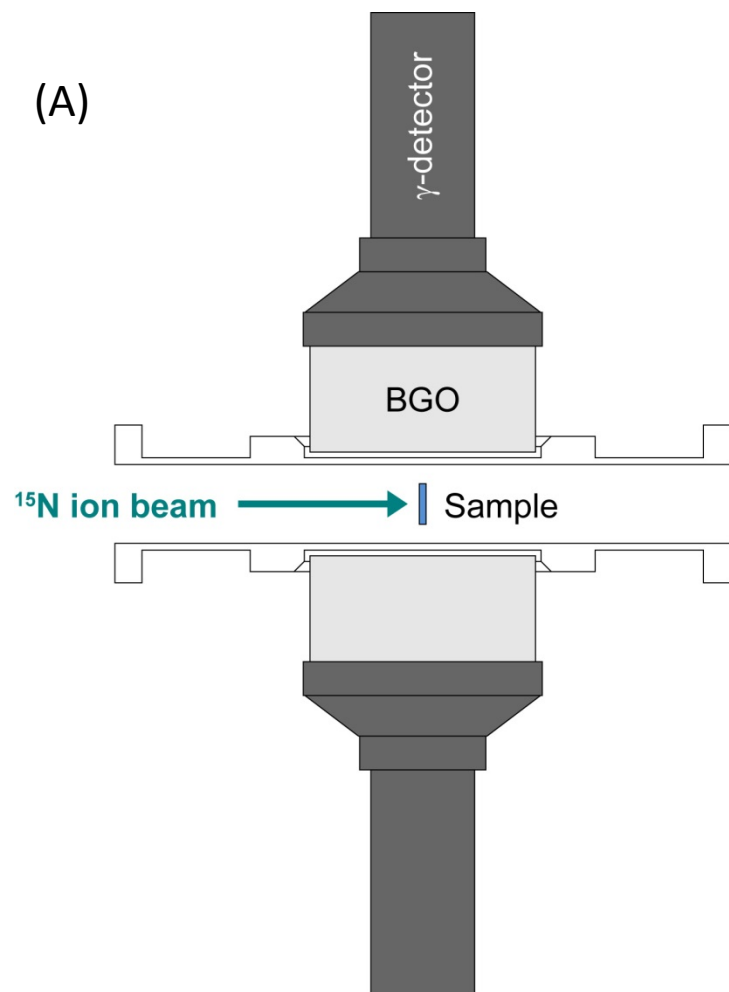


Figure 1



(B)



Figure 2

Figure

[Click here to download Figure: JoVE-NRA-Wilde-Figure3.pdf](#)

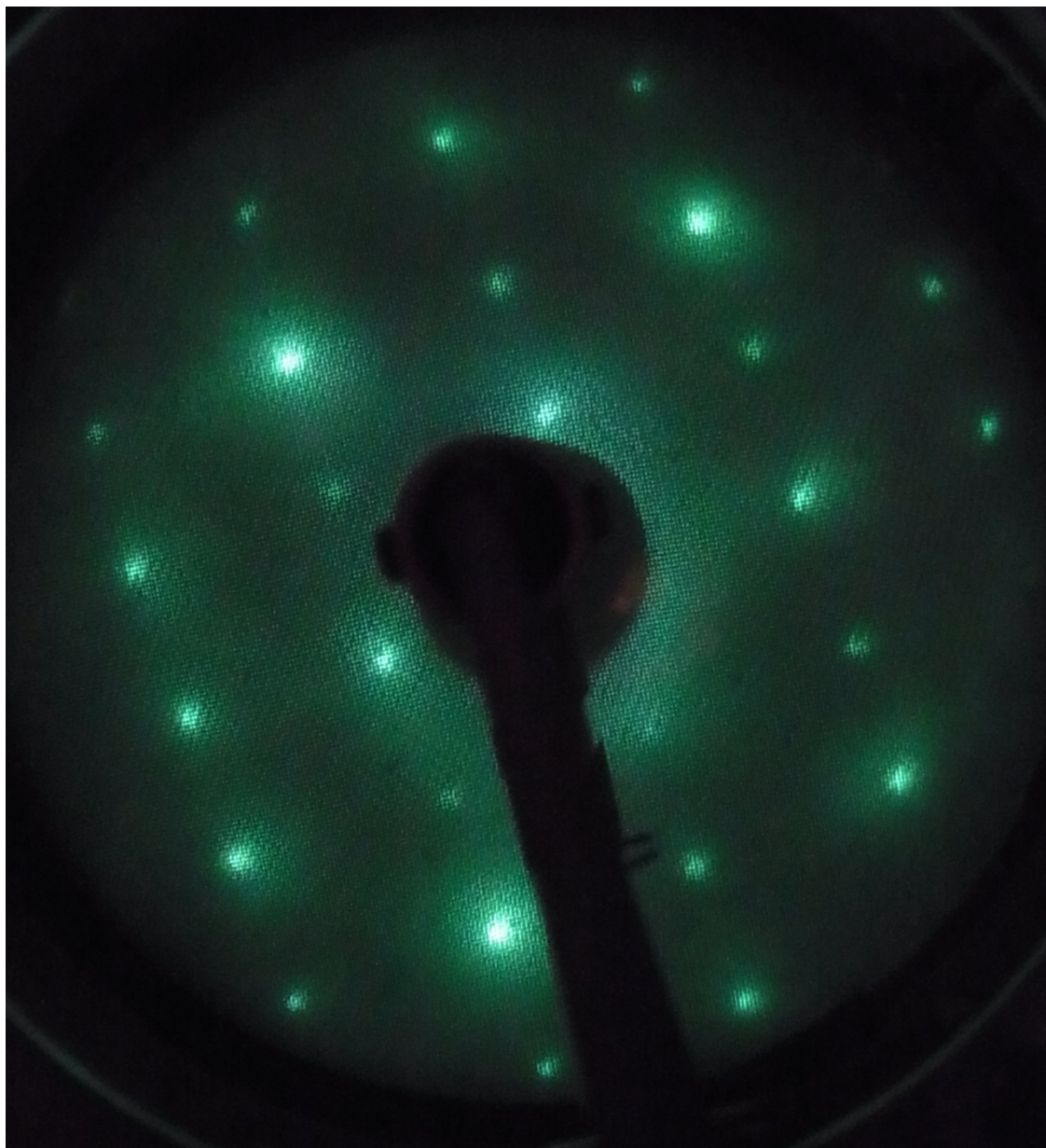


Figure 3

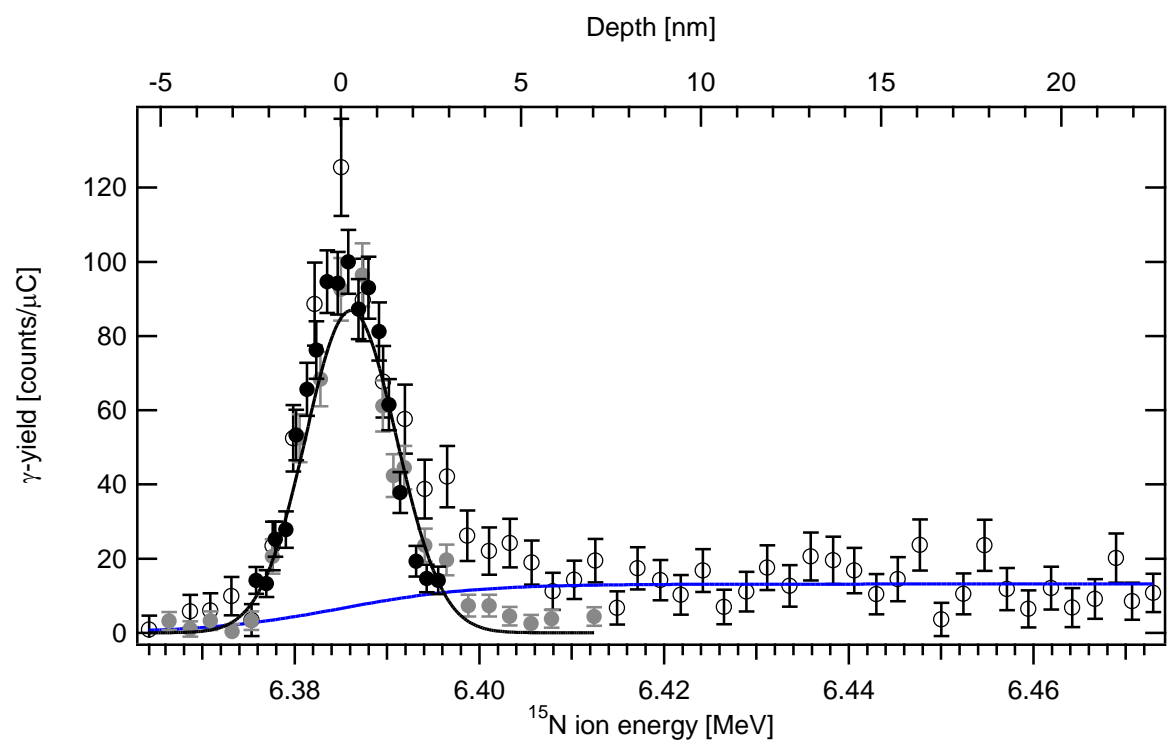


Figure 4

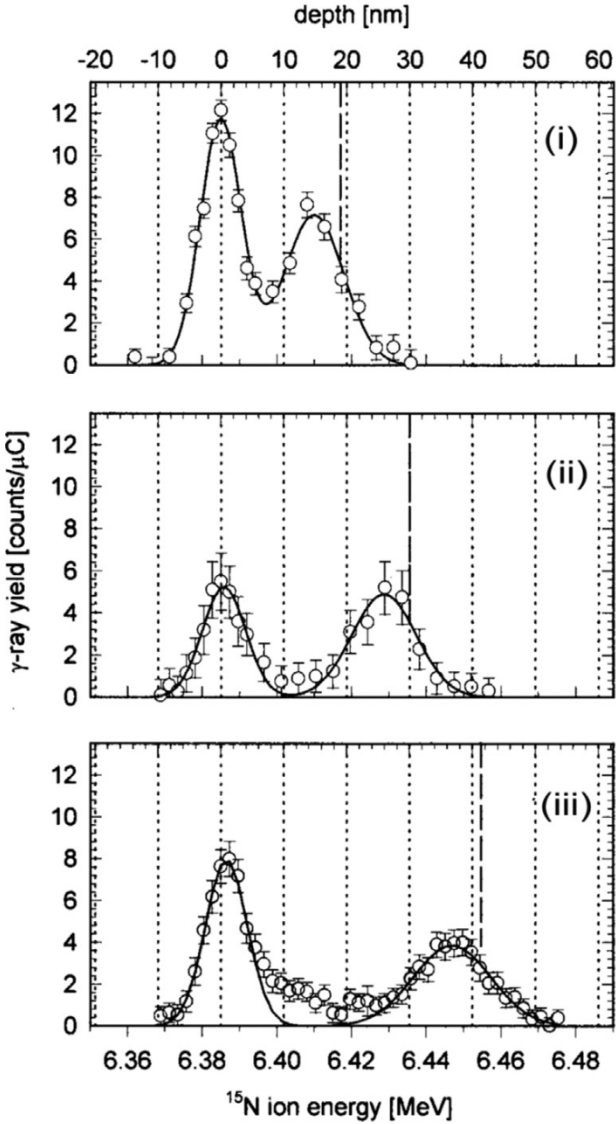


Figure 5

Name of Material	Company	Catalog Number	Comments/Description
Pd single crystal	SPL (Surface Preparation Laboratory), http://www.spl.eu/products.html , or any other suitable supplier	Order made to specification	Disk, 9 mm diam., (110) oriented, aligned to < 0.
H ₂ gas	Joutou Gas Corporation, Ltd., Japan, http://www.jyotougas.co.jp/item/gas.html		(99.9995%), or any other suitable supplier
O ₂ gas	Joutou Gas Corporation, Ltd., Japan, http://www.jyotougas.co.jp/item/gas.html		(99.99%), or any other suitable supplier
Ar gas	Joutou Gas Corporation, Ltd., Japan, http://www.jyotougas.co.jp/item/gas.html		(99.99995%), or any other suitable supplier
Tantalum / Wire	The Nilaco Corporation, http://nilaco.jp/en/oder.php	TA-411325	(99.95%), 0.3 mm diam., or any other suitable su

Alumel / Wire	The Nilaco Corporation, http://nilaco.jp/en/oder.php The Nilaco Corporation, http://nilaco.jp/en/oder.php	851266 0.2 mm diam., or any other suitable supplier
Chromel / Wire (Chromel)	The Nilaco Corporation, http://nilaco.jp/en/oder.php	861266 0.2 mm diam., or any other suitable supplier

5 degree or less, one side polished to $< 0.3 \mu\text{m}$ roughness, self-prepared specimen

ipplier

Name of Equipment	Company	Catalog Number	Comments/Description
3 keV Raster Ion Bombardment Gun and Control	VARIAN, http://www.eurovac.com/docs/varian1.htm OCI, http://www.ocivm.com/spectrometer_bdl800ir.html	981-2046 Power Supply, 981-2043 Ion Gun	or equivalent product of any other suitable manufacturer
LEED-AUGER Optics	Pfeiffer Vacuum, http://www.pfeiffer-vacuum.com/	BDL600IR	or equivalent product of any other suitable manufacturer
Quadrupole Mass Spectrometer	Power + Energy Inc., http://www.powerandenergy.com	Prisma QMS 200	or equivalent product of any other suitable manufacturer
Palladium Hydrogen Purifier		PE-3001	99.9999999% purity; P+E H ₂ purifiers are now built in the USA

ufacturer

ufacturer

ufacturer

usiness of SAES Pure Gases Inc., <http://www.saespuregas.com/Products/Gas-Purifier/Hydrogen/Palladium-Membrane/Palladium-Purifier->

PE2100.html



1 Alewife Center #200
Cambridge, MA 02140
tel. 617.945.9051
www.jove.com

ARTICLE AND VIDEO LICENSE AGREEMENT

Title of Article:

Quantification of Hydrogen Concentrations in Surface and Interface Layers and Bulk Materials through Depth Profiling with Nuclear Reaction Analysis

Author(s):

Martus WILDE, Shohei OGIURA, Katsuyuki Fukutani, Hiroyuki MATSUZAKI

Item 1 (check one box): The Author elects to have the Materials be made available (as described at <http://www.jove.com/publish>) via: ☒ Standard Access ☐ Open Access

Item 2 (check one box):

- ☒ The Author is NOT a United States government employee.
- ☐ The Author is a United States government employee and the Materials were prepared in the course of his or her duties as a United States government employee.
- ☐ The Author is a United States government employee but the Materials were NOT prepared in the course of his or her duties as a United States government employee.

ARTICLE AND VIDEO LICENSE AGREEMENT

1. **Defined Terms.** As used in this Article and Video License Agreement, the following terms shall have the following meanings: “**Agreement**” means this Article and Video License Agreement; “**Article**” means the article specified on the last page of this Agreement, including any associated materials such as texts, figures, tables, artwork, abstracts, or summaries contained therein; “**Author**” means the author who is a signatory to this Agreement; “**Collective Work**” means a work, such as a periodical issue, anthology or encyclopedia, in which the Materials in their entirety in unmodified form, along with a number of other contributions, constituting separate and independent works in themselves, are assembled into a collective whole; “**CRC License**” means the Creative Commons Attribution-Non Commercial-No Derivs 3.0 Unported Agreement, the terms and conditions of which can be found at: <http://creativecommons.org/licenses/by-nc-nd/3.0/legalcode>; “**Derivative Work**” means a work based upon the Materials or upon the Materials and other pre-existing works, such as a translation, musical arrangement, dramatization, fictionalization, motion picture version, sound recording, art reproduction, abridgment, condensation, or any other form in which the Materials may be recast, transformed, or adapted; “**Institution**” means the institution, listed on the last page of this Agreement, by which the Author was employed at the time of the creation of the Materials; “**JoVE**” means MyJoVE Corporation, a Massachusetts corporation and the publisher of *The Journal of Visualized Experiments*; “**Materials**” means the Article and / or the Video; “**Parties**” means the Author and JoVE; “**Video**” means any video(s) made by the Author, alone or in conjunction with any other parties, or by JoVE or its affiliates or agents, individually or in collaboration with the Author or any other parties, incorporating all or any portion of the Article, and in which the Author may or may not appear.

2. **Background.** The Author, who is the author of the Article, in order to ensure the dissemination and protection of the Article, desires to have the JoVE publish the Article and create and transmit videos based on the Article. In furtherance of such goals, the Parties desire to memorialize in this Agreement the respective rights of each Party in and to the Article and the Video.

3. **Grant of Rights in Article.** In consideration of JoVE agreeing to publish the Article, the Author hereby grants to JoVE, subject to **Sections 4 and 7** below, the exclusive, royalty-free, perpetual (for the full term of copyright in the Article, including any extensions thereto) license (a) to publish, reproduce, distribute, display and store the Article in all forms, formats and media whether now known or hereafter developed (including without limitation in print, digital and electronic form) throughout the world, (b) to translate the Article into other languages, create adaptations, summaries or extracts of the Article or other Derivative Works (including, without limitation, the Video) or Collective Works based on all or any portion of the Article and exercise all of the rights set forth in (a) above in such translations, adaptations, summaries, extracts, Derivative Works or Collective Works and (c) to license others to do any or all of the above. The foregoing rights may be exercised in all media and formats, whether now known or hereafter devised, and include the right to make such modifications as are technically necessary to exercise the rights in other media and formats. If the “Open Access” box has been checked in **Item 1** above, JoVE and the Author hereby grant to the public all such rights in the Article as provided in, but subject to all limitations and requirements set forth in, the CRC License.

ARTICLE AND VIDEO LICENSE AGREEMENT

4. Retention of Rights in Article. Notwithstanding the exclusive license granted to JoVE in **Section 3** above, the Author shall, with respect to the Article, retain the non-exclusive right to use all or part of the Article for the non-commercial purpose of giving lectures, presentations or teaching classes, and to post a copy of the Article on the Institution's website or the Author's personal website, in each case provided that a link to the Article on the JoVE website is provided and notice of JoVE's copyright in the Article is included. All non-copyright intellectual property rights in and to the Article, such as patent rights, shall remain with the Author.

5. Grant of Rights in Video – Standard Access. This **Section 5** applies if the "Standard Access" box has been checked in **Item 1** above or if no box has been checked in **Item 1** above. In consideration of JoVE agreeing to produce, display or otherwise assist with the Video, the Author hereby acknowledges and agrees that, Subject to **Section 7** below, JoVE is and shall be the sole and exclusive owner of all rights of any nature, including, without limitation, all copyrights, in and to the Video. To the extent that, by law, the Author is deemed, now or at any time in the future, to have any rights of any nature in or to the Video, the Author hereby disclaims all such rights and transfers all such rights to JoVE.

6. Grant of Rights in Video – Open Access. This **Section 6** applies only if the "Open Access" box has been checked in **Item 1** above. In consideration of JoVE agreeing to produce, display or otherwise assist with the Video, the Author hereby grants to JoVE, subject to **Section 7** below, the exclusive, royalty-free, perpetual (for the full term of copyright in the Article, including any extensions thereto) license (a) to publish, reproduce, distribute, display and store the Video in all forms, formats and media whether now known or hereafter developed (including without limitation in print, digital and electronic form) throughout the world, (b) to translate the Video into other languages, create adaptations, summaries or extracts of the Video or other Derivative Works or Collective Works based on all or any portion of the Video and exercise all of the rights set forth in (a) above in such translations, adaptations, summaries, extracts, Derivative Works or Collective Works and (c) to license others to do any or all of the above. The foregoing rights may be exercised in all media and formats, whether now known or hereafter devised, and include the right to make such modifications as are technically necessary to exercise the rights in other media and formats. For any Video to which this Section 6 is applicable, JoVE and the Author hereby grant to the public all such rights in the Video as provided in, but subject to all limitations and requirements set forth in, the CRC License.

7. Government Employees. If the Author is a United States government employee and the Article was prepared in the course of his or her duties as a United States government employee, as indicated in **Item 2** above, and any of the licenses or grants granted by the Author hereunder exceed the scope of the 17 U.S.C. 403, then the rights granted hereunder shall be limited to the maximum rights permitted under such

statute. In such case, all provisions contained herein that are not in conflict with such statute shall remain in full force and effect, and all provisions contained herein that do so conflict shall be deemed to be amended so as to provide to JoVE the maximum rights permissible within such statute.

8. Likeness, Privacy, Personality. The Author hereby grants JoVE the right to use the Author's name, voice, likeness, picture, photograph, image, biography and performance in any way, commercial or otherwise, in connection with the Materials and the sale, promotion and distribution thereof. The Author hereby waives any and all rights he or she may have, relating to his or her appearance in the Video or otherwise relating to the Materials, under all applicable privacy, likeness, personality or similar laws.

9. Author Warranties. The Author represents and warrants that the Article is original, that it has not been published, that the copyright interest is owned by the Author (or, if more than one author is listed at the beginning of this Agreement, by such authors collectively) and has not been assigned, licensed, or otherwise transferred to any other party. The Author represents and warrants that the author(s) listed at the top of this Agreement are the only authors of the Materials. If more than one author is listed at the top of this Agreement and if any such author has not entered into a separate Article and Video License Agreement with JoVE relating to the Materials, the Author represents and warrants that the Author has been authorized by each of the other such authors to execute this Agreement on his or her behalf and to bind him or her with respect to the terms of this Agreement as if each of them had been a party hereto as an Author. The Author warrants that the use, reproduction, distribution, public or private performance or display, and/or modification of all or any portion of the Materials does not and will not violate, infringe and/or misappropriate the patent, trademark, intellectual property or other rights of any third party. The Author represents and warrants that it has and will continue to comply with all government, institutional and other regulations, including, without limitation all institutional, laboratory, hospital, ethical, human and animal treatment, privacy, and all other rules, regulations, laws, procedures or guidelines, applicable to the Materials, and that all research involving human and animal subjects has been approved by the Author's relevant institutional review board.

10. JoVE Discretion. If the Author requests the assistance of JoVE in producing the Video in the Author's facility, the Author shall ensure that the presence of JoVE employees, agents or independent contractors is in accordance with the relevant regulations of the Author's institution. If more than one author is listed at the beginning of this Agreement, JoVE may, in its sole discretion, elect not take any action with respect to the Article until such time as it has received complete, executed Article and Video License Agreements from each such author. JoVE reserves the right, in its absolute and sole discretion and without giving any reason therefore, to accept or decline any work submitted to JoVE. JoVE and its employees, agents and independent contractors shall have

ARTICLE AND VIDEO LICENSE AGREEMENT

full, unfettered access to the facilities of the Author or of the Author's institution as necessary to make the Video, whether actually published or not. JoVE has sole discretion as to the method of making and publishing the Materials, including, without limitation, to all decisions regarding editing, lighting, filming, timing of publication, if any, length, quality, content and the like.

11. **Indemnification.** The Author agrees to indemnify JoVE and/or its successors and assigns from and against any and all claims, costs, and expenses, including attorney's fees, arising out of any breach of any warranty or other representations contained herein. The Author further agrees to indemnify and hold harmless JoVE from and against any and all claims, costs, and expenses, including attorney's fees, resulting from the breach by the Author of any representation or warranty contained herein or from allegations or instances of violation of intellectual property rights, damage to the Author's or the Author's institution's facilities, fraud, libel, defamation, research, equipment, experiments, property damage, personal injury, violations of institutional, laboratory, hospital, ethical, human and animal treatment, privacy or other rules, regulations, laws, procedures or guidelines, liabilities and other losses or damages related in any way to the submission of work to JoVE, making of videos by JoVE, or publication in JoVE or elsewhere by JoVE. The Author shall be responsible for, and shall hold JoVE harmless from, damages caused by lack of sterilization, lack of cleanliness or by contamination due to the making of a video by JoVE its employees, agents or independent contractors. All sterilization, cleanliness or decontamination procedures shall be solely the responsibility of the Author and shall be undertaken at the Author's

expense. All indemnifications provided herein shall include JoVE's attorney's fees and costs related to said losses or damages. Such indemnification and holding harmless shall include such losses or damages incurred by, or in connection with, acts or omissions of JoVE, its employees, agents or independent contractors.

12. **Fees.** To cover the cost incurred for publication, JoVE must receive payment before production and publication of the Materials. Payment is due in 21 days of invoice. Should the Materials not be published due to an editorial or production decision, these funds will be returned to the Author. Withdrawal by the Author of any submitted Materials after final peer review approval will result in a US\$1,200 fee to cover pre-production expenses incurred by JoVE. If payment is not received by the completion of filming, production and publication of the Materials will be suspended until payment is received.

13. **Transfer, Governing Law.** This Agreement may be assigned by JoVE and shall inure to the benefits of any of JoVE's successors and assignees. This Agreement shall be governed and construed by the internal laws of the Commonwealth of Massachusetts without giving effect to any conflict of law provision thereunder. This Agreement may be executed in counterparts, each of which shall be deemed an original, but all of which together shall be deemed to be one and the same agreement. A signed copy of this Agreement delivered by facsimile, e-mail or other means of electronic transmission shall be deemed to have the same legal effect as delivery of an original signed copy of this Agreement.

A signed copy of this document must be sent with all new submissions. Only one Agreement required per submission.

CORRESPONDING AUTHOR:

Name:

Markus WILDE

Department:

Institute of Industrial Science

Institution:

The University of Tokyo

Article Title:

Quantification of Hydrogen Concentrations in Surface and Interface Layers and Bulk Materials through Depth Profiling with Nuclear Reaction Analysis

Signature:

Markus Wilde

Date:

3/20/2015

Please submit a signed and dated copy of this license by one of the following three methods:

- 1) Upload a scanned copy of the document as a pdf on the JoVE submission site;
- 2) Fax the document to +1.866.381.2236;
- 3) Mail the document to JoVE / Attn: JoVE Editorial / 1 Alewife Center #200 / Cambridge, MA 02139

For questions, please email submissions@jove.com or call +1.617.945.9051

JoVE 53452_R2: Reply to Editorial and Reviewers' comments

Editorial comments:

Changes to be made by the Author(s):

1. Please take this opportunity to thoroughly proofread the manuscript to ensure that there are no spelling or grammar issues. The JoVE editor will not copy-edit your manuscript and any errors in the submitted revision may be present in the published version.

→ *We proofread the manuscript carefully and made several small amendments (changes are highlighted in the text).*

2. Please define the error bars in Figure 4 and 5 in the appropriate Figure Legend.

→ *We added to the Legends of Figures 4 and 5 a reference to the error bar calculation formalism, which is given as a Note in Procedure Step 6.8. We do not consider it helpful repeating the formalism itself in the Figure Legends, because defining all entering quantities would render those captions unnecessarily lengthy.*

3. Please provide a complete reference for Reference 29, 31.

→ *Ref. 29 cites historically important fundamental work by Niels Bohr on electronic stopping of high energy ions in matter, published in a Danish journal on mathematical physics. This classic paper is frequently cited by the ion beam physics community in the exact form that I provided in the JoVE manuscript. Due to its age, no electronic version of the article (hence no DOI) exists to my knowledge. Therefore, please kindly understand that that Ref. 29 cannot further be 'completed'.*

→ *Ref. 31 is the link to the website of the MALT accelerator facility, where application procedures are documented and application forms can be downloaded for potential users of the facility. Please explain what further 'completion' should be necessary here?*

4. Please confirm that we will be able to access all relevant parts of the facility.

→ *I confirm that the filming team will have access to all the relevant sections of the MALT accelerator facility. That being said, it will be necessary to schedule the filming during a time when the accelerator facility has assigned machine time to our group (Fukutani-Wilde Laboratory) for NRA measurements. Only during such times (typically 4-5 times per year for about one week) our group has access to the beamlines and we are able to use the accelerator for NRA measurements. The next opportunity to do so is a machine time from **August 12 to August 21, 2015**. The next machine time cannot be expected before October or November 2015. To proceed publication of our video article, I therefore suggest scheduling the filming during the upcoming August machine time. Please kindly consider whether a JoVE filming set can be arranged in this period.*

Reviewers' comments:

Reviewer #1:

The authors present a manuscript describing the protocol for nuclear reaction analysis at the MALT Tandem accelerator facility of the university of Tokyo. The procedure is known to be sensitive to the concentration of hydrogen atoms in the vicinity of surfaces. The potential of the method is demonstrated for a palladium surface and for SiO₂ thin films deposited on silicon.

The manuscript is well written and concise. The procedure is explained in detail and it is expected to reproduce the desired outcome. Nonetheless, some steps could benefit from a better explanation, in particular those concerning the participation of the assisting scientist:

"Tighten flange bolts and evacuate UHV system following instructions from the assisting scientist." (line 275) "Obtain instructions from the assisting scientist to become familiar with the accelerator control system in the control room." (line 346)

→ *a) We gratefully appreciate the Reviewer's careful reading and generally positive evaluation. We consider the particular instructions on the vacuum chamber evacuation (line 275) and operation of the accelerator control system (line 346) as highly facility-specific. Their description would require considerable additional text length but should be of little interest to most readers who may want to learn about the NRA technique in principle. We are prepared to support any collaborating scientist who may actually want to perform NRA measurements at our facility by making the additional instructions requested by the Reviewer available, but expect that this will only concern a tiny fraction of the article's potential readership. With regard to manuscript length and readability, we would therefore prefer not to include also these details in the paper, although other (arguably equally technical) details have been given in the procedures (see also our reply to the last comment by Reviewer #1). The NOTE in lines 349-351 at least provides a brief principal description of the MALT control system. Actions performed with this control system will also be filmed and appear in the video that accompanies our article, so we believe that together with the video sufficient information is provided to form an adequately detailed impression of the protocol.*

Also, in section 5 (NRA Measurement at BL-2C), the acquisition time is not mentioned. From the introduction, I am lead to believe that the acquisition time should be shorter that at in the previous section (50 s).

→ *b) We thank the Reviewer for pointing out this significant shortcoming. We added the acquisition time setting for the NRA Measurement at BL-2C (for SiO₂/Si) to the protocol (Step 5.2), and also provided a recommendation for the intensity of the ¹⁵N ion beam (50-100 nA on FC04) in Step 5.3. These parameters are determined by the requirement to obtain sufficient NRA γ -ray yield from the given H density in the target sample to achieve satisfactory counting statistics. In the present case, because the surface and interfacial H layer densities in the SiO₂/Si targets are about one order of magnitude smaller than in the saturated surface H layer on Pd(110), the acquisition time in the described BL-2C*

measurement has actually been the same as in BL-1E, not shorter, despite higher sensitivity in BL-2C. We added an explanation of this situation to the discussion (lines 704-709 in the revised manuscript).

From a physical point of view, the method is presented clearly and I find particularly refreshing that the authors are not trying to oversell it. It could nonetheless be beneficial to add a few more words concerning the spatial resolution of the technique, especially for metallic systems. In the text at lines 548-551, the H-uptake in the interfacial region is simply fitted to a sigmoid, whereas Figure 4 exhibits some corrugation. Is it possible to extract more information from this corrugation?

→ *We have very good reason to believe that the corrugation in Figure 4 results from background fluctuations in our γ -detection system rather than reflecting real concentration gradients in the H depth distribution in the Pd single crystal. We added these reasons and further explanations of the near-surface depth resolution to the discussion in lines 552-562 (revised manuscript) and thereby explained to the reader why our use of the sigmoid fit function is justified:*

“Figure 4 also shows that the depth resolution of the NRA H profile in the near-surface region is limited by the width of the surface resonance peak to about 2-3 nm (\approx FWHM/S). Therefore, any abrupt features in the H profile such as the point-to-point γ -yield variations around 16 nm depth cannot correspond to actually existing steep H concentration gradients, because such would be smeared out by the surface peak width and additional energy broadening due to ^{15}N ion straggling³. Hence, the γ -yield corrugations in the plateau region of the H profile (5 to 22 nm depth) reflect fluctuations of the BGO background count rate (separate background measurements confirm that such random fluctuations occur) and do not contain physical information on the depth distribution of the Pd-absorbed hydrogen. The latter distribution is expected to be rather smooth in the homogenous single crystal, where H diffusion is rapid (several 100 nm/s even at 145 K)^{3, 13, 15}. Thus, the approximately constant concentration of the bulk-absorbed hydrogen in the near-surface region of the Pd crystal after exposure to 2000 L H_2 at 145 K can be evaluated by fitting the plateau data in Figure 4 to a sigmoid function that rises to its half-height at E_{res} with the same width as the Gaussian surface peak. ...”

Also, a discussion of the time resolution of the procedure could be included. Is it possible to investigate the transient evolution of a system and, if so, on which timescales?

→ *Yes, it is possible to observe transient evolutions of H densities with NRA, such as upon adsorption, desorption, absorption, or diffusion of hydrogen in target materials, on the time scale defined by the acquisition time. We added a brief description of these circumstances to the discussion in lines 709-711.*

The main critique to the manuscript is that the procedure appears to be valid only in a single facility. Then again, this is probably a necessary requirement for describing the methodology used in such detail.

→ *In this and also his first comment, Reviewer #1 points out a ‘dilemma’ that also we felt during authoring the article. The unique JoVE format puts much focus on the experimental procedure. Thus, the methodology has to be described in quite some technical detail to enable reproduction of the results on*

one hand, yet of course the article should still remain readable and generally informative to a wider audience, on the other. Especially because our particular method involves an accelerator and custom design experimental stations, many procedure steps are necessarily facility-specific. We are afraid that this cannot be helped, but hope nonetheless that our descriptions will enable the reader to extract the experimental principles of the NRA technique and to potentially extrapolate from these to situations in other laboratories. We have strived to maintain a reasonable balance between facility-specific detail and explanation of the principle ways of the experiment in the article, and our deliberate omission of, e.g., evacuation steps of a specific vacuum system and detailed descriptions of the controls at MALT were meant as ways to preserve this balance.

Reviewer #2:

1. One point that is not mentioned that can be important is the beam spot size (or beam intensity in (beam current)/cm²). Unlike most other elements undergoing MeV ion beam analysis, H can be lost during analysis limiting the application of this method to materials in which the H is only weakly bound. With the same beam current, if the beam spot is 1 mm by 1 mm, the same beam current with a 1 cm by 1 cm beam spot has 100 time less beam intensity, making analysis of even very delicate materials possible.

→ We thank the Reviewer for pointing out an important point. Following his suggestion, we have provided a more detailed explanation of possible beam-induced H loss from the target material and included mentioning of the possibility to reduce such effects by defocusing the ion beam in the discussion (lines 666-676 of the revised manuscript):

“The tendency of H to desorb from the sample or to redistribute inside the target by diffusion under the ion beam varies strongly between different target materials and should be evaluated as part of any given analysis by monitoring the γ -yield at the probing depth of interest as a function of the ion beam dose. Without a compensating H₂ background as applied here to Pd(110) where H readsorbs readily, in many cases a more or less pronounced exponential decay of the H-signal can be observed. Measuring and extrapolating such H-loss functions to zero ¹⁵N exposure allows reproducing the original H density on or inside the target prior to perturbation by the ion beam (for details, see Ref. 3). If the target size permits, reducing the current density (nA/cm²) in the beam-irradiated surface spot by defocusing the ion beam with aid of the MQ04 magnetic lenses (Protocol Steps 2.3.5 and 3.10) may alleviate H losses during the analysis.”

2. The authors don't seem to say how they established the absolute calibration of the method. For anyone wanting to establish this method in their own laboratory, this is a key step usually accomplished by measuring samples with well known H content (either bulk or ion implanted).

→ We actually did mention the sensitivity calibration using a Kapton foil concentration standard in line 542 (original manuscript), but this admittedly very brief and embedded text may have failed to catch the reviewer's attention. To describe the calibration procedure more explicitly, we added a few more details in lines 545-546 and 568-569 of the revised manuscript.

3. I don't think a viewer (reader) needs to know all the local accelerator/data collection protocols. They are specific to that particular institution.

→ *We would agree with the Reviewer's assertion, but are afraid that the JoVE's focus on the experimental procedure makes it inevitable to include a fair amount of technical detail that (especially in case of our particular accelerator-based method) is facility-specific. Please also refer to our reply to a similar remark by Reviewer #1.*

4. I have no doubt that the examples shown to demonstrate the method are correct. The examples illustrate some of the important types of application of ^{15}N hydrogen profiling.

→ *We thank the reviewer for this positive assessment.*

Supplemental File (as requested by JoVE)

[Click here to download Supplemental File \(as requested by JoVE\): Rightslink Printable License.pdf](#)

Scripwriter_Guide-Photos

[Click here to download Supplemental File \(as requested by JoVE\): JoVE-NRA-Orientation.pptx](#)

Supplemental File (as requested by JoVE)

[Click here to download Supplemental File \(as requested by JoVE\): 53452_Filmed Steps.docx](#)